Biomaterials 76 (2016) 33–51

Contents lists available at ScienceDirect

Biomaterials

journal homepage: www.elsevier.com/locate/biomaterials

Chitosan-film enhanced chitosan nerve guides for long-distance regeneration of peripheral nerves

Cora Meyer [a, 1], Lena Stenberg [b, 1], Francisco Gonzalez-Perez [c, 1], Sandra Wrobel [a], Giulia Ronchi [e], Esther Udina [c], Seigo Suganuma [d], Stefano Geuna [e], Xavier Navarro [c], Lars B. Dahlin [b], Claudia Grothe [a, *, 2], Kirsten Haastert-Talini [a, 2]

[a] Institute of Neuroanatomy, Hannover Medical School, Hannover, Germany and Center for Systems Neuroscience (ZSN), Hannover, Germany
[b] Department of Translational Medicine – Hand Surgery, Lund University, Skåne University Hospital, Malmö, Sweden
[c] Department of Cell Biology, Physiology, and Immunology, Institute of Neurosciences, Universitat Autonoma de Barcelona and CIBERNED, Bellaterra, Spain
[d] Department of Orthopaedic Surgery, Kanazawa University Hospital, Kanazawa, Japan
[e] Department of Clinical and Biological Sciences, and Cavalieri Ottolenghi Neuroscience Institute, University of Turin, Turin, Italy

ARTICLE INFO

Article history:
Received 27 August 2015
Received in revised form
13 October 2015
Accepted 18 October 2015
Available online 21 October 2015

Keywords:
Chitosan film
Chitosan nerve guide
Regenerative matrix
Functional recovery
Nerve morphometry
Diabetic condition

ABSTRACT

Biosynthetic nerve grafts are developed in order to complement or replace autologous nerve grafts for peripheral nerve reconstruction. Artificial nerve guides currently approved for clinical use are not widely applied in reconstructive surgery as they still have limitations especially when it comes to critical distance repair. Here we report a comprehensive analysis of fine-tuned chitosan nerve guides (CNGs) enhanced by introduction of a longitudinal chitosan film to reconstruct critical length 15 mm sciatic nerve defects in adult healthy Wistar or diabetic Goto-Kakizaki rats. Short and long term investigations demonstrated that the CNGs enhanced by the guiding structure of the introduced chitosan film significantly improved functional and morphological results of nerve regeneration in comparison to simple hollow CNGs. Importantly, this was detectable both in healthy and in diabetic rats (short term) and the regeneration outcome almost reached the outcome after autologous nerve grafting (long term). Hollow CNGs provide properties likely leading to a wider clinical acceptance than other artificial nerve guides and their performance can be increased by simple introduction of a chitosan film with the same advantageous properties. Therefore, the chitosan film enhanced CNGs represent a new generation medical device for peripheral nerve reconstruction.

1. Introduction

Treatment of peripheral nerve transection and laceration injuries represents a major challenge in reconstructive surgery and regenerative medicine. Although peripheral nerves are featured with the intrinsic capacity to regenerate, the degree of functional recovery depends on a number of factors, such as the patient's age and general condition, the type of nerve, the delay between the accident causing the injury and the time of surgery, the skills of the surgeon as well as on the location and length of the nerve injury. Small defects (<2 cm) between the separated nerve ends in humans can be bridged by a number of marketed bioartificial hollow conduits of various origins or by processed human peripheral nerve tissue from donors [1]. Treatment of larger defects, however, is still a field of intensive research with the autologous nerve graft treatment representing the clinical gold standard [2,3]. For the latter, the grafts are harvested from less important sensory nerves. Regeneration and functional recovery across defects of >3 cm in length, however, are often incomplete due to differences in nerve architecture (e.g. size of endoneurial tubes) and mismatch in Schwann cell phenotypes (sensory vs motor nerve peripheral glia cells) [4].

* Corresponding author. Institute of Neuroanatomy, Hannover Medical School, Carl-Neuberg-Str.1, 30625, Hannover, Germany.
E-mail address: Grothe.Claudia@mh-hannover.de (C. Grothe).

[1] Cora Meyer, Lena Stenberg, and Francisco Gonzalez-Perez share first authorship as they performed substantial parts of either study III, study II, and study I. They analyzed the data. CM collected and arranged the data for the first draft of the manuscript.

[2] Kirsten Haastert-Talini and Claudia Grothe share senior authorship. KHT coordinated the experiments, outlined the manuscript and wrote its final version. CG initiated the experiments, contributed to the study concept and to drafting of the final manuscript.

http://dx.doi.org/10.1016/j.biomaterials.2015.10.040

Furthermore, this type of treatment has several disadvantages, including donor site morbidity, need of additional surgery and limited number of available grafts [3,5]. Another condition that can limit the outcome of any chosen reconstructive therapy for injured peripheral nerves is generalized peripheral neuropathy, such as that occurring in diabetes [6]. The number of patients with diabetes is increasing globally and any innovative technique for peripheral nerve repair and reconstruction needs to be evaluated not only for the use in subjects with healthy general conditions, but also for those with diabetes [6,7]. Current research and development attempts aim therefore to overcome the present obstacles that prevent a widespread use of bioartificial nerve guides, to significantly increase the length limit that can currently be successfully bridged with them (max 2.5 cm) [8], and to significantly improve the achievable level of functional recovery both in generally healthy and diabetic subjects suffering from traumatic nerve injuries. The usually accepted maximal defect length for nerve guide repair in the clinic is 2.5 cm because the surgeon needs to ensure that regeneration will occur also without the use of autologous nerve transplantation. The clinical use of nerve guides, however, depends also on the type of nerve that has to be reconstructed, e.g., small digital nerves or the larger median or ulnar nerves [9–11]. To overcome the critical gap lengths, many different attempts have been evaluated experimentally also in larger animal models like Beagle dogs with a defect lengths of 3–6 cm [12–14].

We have previously demonstrated that hollow nerve guides produced from a fine-tuned form of the natural biopolymer chitosan are as effective in peripheral nerve repair as autologous nerve grafts when bridging 10 mm sciatic nerve gaps in rat experimental models [15–17]. These nerve guides did further qualify for functional repair of critical length, 15 mm, sciatic nerve defects in a considerably high percentage of the evaluated rats [18]. In order to further increase the regeneration outcome, the chitosan nerve guides have been filled with a neural and vascular regenerative hydrogel (NVR-Gel) in a non-modified form or additionally enriched with primary, naïve or genetically modified Schwann cells overexpressing selected neurotrophic factors. Although supporting neurite outgrowth in vitro, the NVR-Gel did not provide a growth-permissive environment in vivo, but rather impaired the regeneration process across a 15 mm critical defect. Supplementation of fibroblast growth factor 2 (FGF-2) overexpressing Schwann cells was able to partially overcome this obstacle [19].

The aim of the present study was to apply a simpler intraluminal modification to the chitosan nerve guides in order to increase the success of axonal regeneration and enhance functional recovery across the critical defect length of 15 mm in rat sciatic nerves in healthy and diabetic rats; the latter with moderate and clinically relevant blood glucose levels and with a profile resembling type 2 diabetes [6]. We enhanced the chitosan nerve guides by introducing a longitudinal film made out of the same fine-tuned chitosan. That a longitudinal guidance structure can increase peripheral nerve regeneration has earlier been demonstrated [20]. The chitosan film that we used for the purpose of chitosan tube enhancement has previously demonstrated to be a suitable biomaterial for Schwann cell attachment and support of sensory dorsal root ganglion neurite outgrowth in vitro [21].

The potential of chitosan film enhanced chitosan nerve guides (CFeCNG) to increase peripheral nerve regeneration was evaluated in three coordinated successive sub-studies. Study I compared the functional and morphological outcome of peripheral nerve regeneration after 15 mm sciatic nerve defect reconstruction with hollow chitosan nerve guides (hCNG) or 1st generation CFeCNG (continuous chitosan films). In the next step the chitosan films were modified by introducing holes allowing exchange between the two compartments of 2nd generation CFeCNG and comprehensive short (Study II) and long-term (Study III) studies were conducted. Study II evaluated the initially formed regenerated matrix within hCNGs or CFeCNGs and the regeneration related processes within the dorsal root ganglia at 56 days after surgery with immunohistochemical methods. These crucial early events of regeneration were additionally addressed regarding the differences between generally healthy and diabetic rats. Study III finally evaluated comprehensively the functional and morphological outcome of peripheral nerve regeneration in experimental groups including implantation of (i) hCNG and (ii) 2nd generation CFeCNG, additionally compared to (iii) autologous nerve grafts (ANGs) and (iv) CFeCNG enriched with FGF-2 overexpressing Schwann cells (SC-FGF-2^{18kDa}). Two very important results were achieved in our comprehensive analyses. First, motor recovery was detectable in significantly more animals in CFeCNG groups than in hCNG groups and the 2nd generation CFeCNG group demonstrated a significantly better outcome in this respect than the 1st generation CFeCNG group. While in the ANG group 100% of the animals demonstrated reinnervation of proximal as well as distal target muscles this was reached in the remarkable amount of 86% and 67% of the CFeCNG^{2nd} group. Second, and similarly important, 2nd generation CFeCNGs supported the early regenerative process more than hCNGs and this was particularly relevant in diabetic rats.

2. Materials and methods

2.1. Manufacturing of chitosan film enhanced chitosan nerve guides (CFeCNG)

Pandalus borealis shrimp shells served as a source for certified medical grade chitosan (Altakitin S.A., Lisboa, Portugal). Hollow chitosan nerve guides (hCNG) with an inner diameter of 2.1 mm and a length of 19 mm as well as chitosan films (CF) were manufactured as described before (Chitosan degree of acetylation ~ 5%; [15,21]) at Medovent GmbH (Mainz, Germany). ISO 13485 requirements and specifications were applied for all production steps.

The CFs were cut into a rectangular shape of 15 mm length and 5 mm width. To allow insertion into the conduits, CFs were folded into a Z-form along their longitudinal axis resulting in kinked edges of 1.5 mm width pointing into opposite directions (Fig. 1A). Before being sterilized by electron beam, these films were placed in the center of chitosan nerve guides leaving 2 mm on each side for nerve end insertion and suturing (Fig. 1B, 1st generation of CFeCNG). For production of 2nd generation CFeCNGs (Fig. 1C–D), six holes were introduced along the middle line of the CFs at a distance of 2 mm between each other by using a sharp needle (0.30 × 12 mm). Introduction of the holes was performed in an alternating manner from both sides to provide similar surface properties at the two compartments of the CFeCNG.

2.2. Experimental design

Table 1 summarizes the three coordinated successive sub-studies performed and provides an overview regarding the respective experimental groups as well as accomplished analyses after 15 mm rat sciatic nerve defect reconstruction. Study I was conducted at the Universitat Autònoma de Barcelona (UAB, Spain) and included two reconstruction conditions: basic hCNGs (group hCNG-I) or 1st generation CFeCNGs (group CFeCNG^{1st}). The observation period was 122 days in which functional recovery was periodically assessed. Study II was executed at University of Lund (ULUND, Sweden) and included two reconstruction conditions in generally healthy or diabetic Goto-Kakizaki rats [6]: basic hCNGs or 2nd generation CFeCNGs (groups: hCNG-II^{healthy}, hCNG-II^{diabetic};

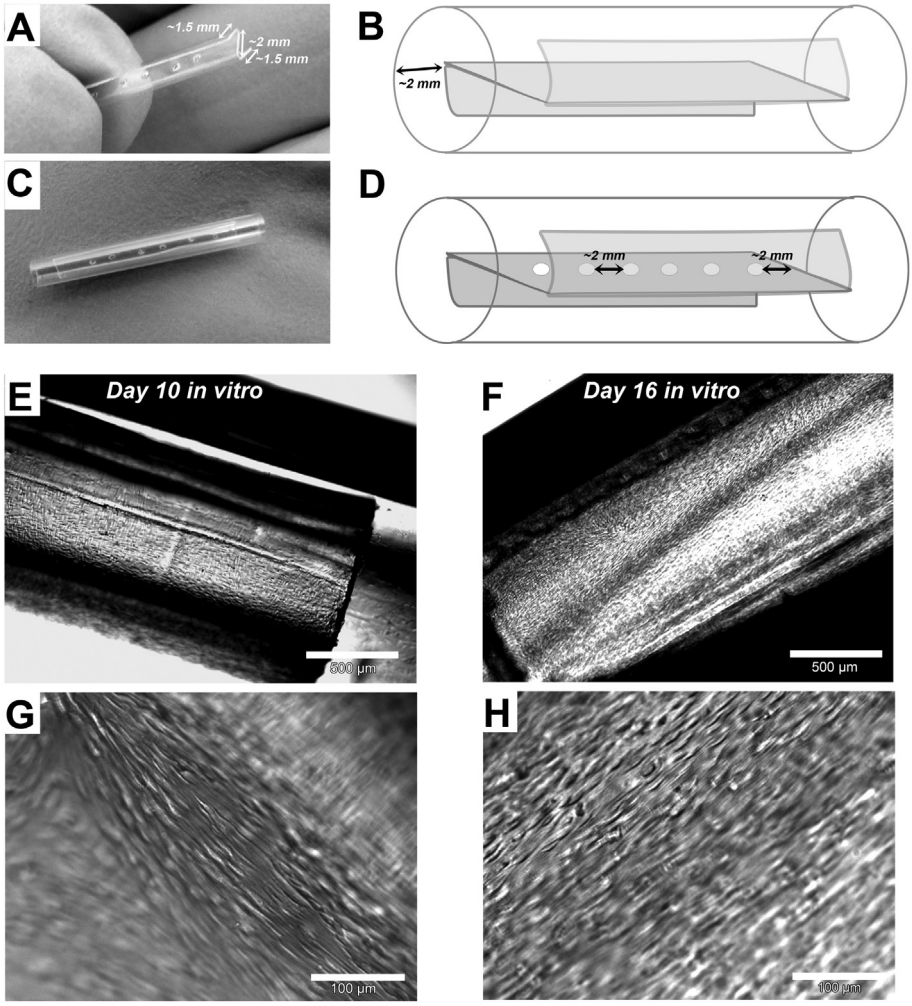

Fig. 1. Preparation of the different types of nerve guides used. (A) Chitosan films were cut into rectangular shape (length: 15 mm, width: 5 mm) and manually folded into a Z-form. (B–D) Film placement within basic chitosan conduits (length: 19 mm, inner diameter: 2.1 mm) left about 2 mm space at both ends to allow nerve end insertion and suturing. (B) 1st generation chitosan film enhanced chitosan nerve guide (CFeCNG) as used in study I. (C–D) 2nd generation CFeCNGs as used in study II and study III with six holes 2 mm distant from each other. (E–F) Representative photomicrographs taken from CFeCNG^{2nd} seeded with neonatal rat Schwann cells. Top views on a nerve guide after 10 days in vitro (E) or after 16 days in vitro (F). (G–H) Detail of the Schwann cell seeded chitosan films within the nerve guides illustrating the fish-swarm like growth of the Schwann cells on both surfaces of the films after 10 days in vitro (G) or 16 days in vitro (H).

CFeCNG$^{2nd\text{-}healthy}$; CFeCNG$^{2nd\text{-}diabetic}$). The observation period, based on pilot experiments, was 56 days in order to assess the formed regenerative matrix, axonal outgrowth, Schwann cell activation and apoptosis, as well as activation and neuroprotection of sensory dorsal root ganglion neurons with immunohistological techniques. Study III was performed at Hannover Medical School (MHH, Germany) and included four reconstruction conditions: autologous nerve grafts (group ANG), basic hCNGs (group hCNG-III), 2nd generation CFeCNGs (group CFeCNG^{2nd}), and 2nd generation CFeCNGs enriched with FGF-2^{18kDa} overexpressing Schwann cells (SCs) seeded on both sides of the CF (group CFeCNG^{2nd}-SC-FGF-2^{18kDa}). The observation period was 120 days in which functional recovery was periodically assessed. Study I and Study III were completed by endpoint histomorphometrical analysis of axonal regeneration.

2.3. Animals and surgery

The in vivo studies were performed in three different laboratories as stated above with different animal breeders and regimes for anesthesia and analgesia due to different local animal care rules. All animal experiments were approved by the local animal ethical committees (animal ethics committee in Malmö [ULUND, Sweden], Barcelona [UAB, Spain], and Lower-Saxony [MHH, Germany]). In common, female Wistar rats (225–250 g) and Goto-Kakizaki rats (GK-rats: kindly provided by Malin Fex, Lund University; around 250 g) were subjected to the experiments and housed in groups of four animals under standard conditions, with food and water ad libitum (the diabetic GK rats were provided with extra water). Fasting blood sugar was measured once a week in the rats at ULUND from the tail vein (Ascensia contour TM [Bio health Care, USA, Bio Diagnostics Europe] and LT [Bayer AB, Diabetes Care, Solna, Sweden]; test slips Microfil TM [Bio Healthcare Diabetes Care, USA]).

Aseptic conditions, sufficient anesthesia and analgesia were applied for all surgical procedures and postoperative analgesia was ensured by appropriate drug application. Animals were prepared and underwent surgery as described before [15,18]. Briefly, following exposure at midthigh level, the left sciatic nerve was transected by a single microscissor cut at a constant point (6 mm distal to its exit from the gluteus muscle) and a 6 mm segment removed from the distal nerve end in study I. In studies II and III

Table 1
Overview of the experimental design of the three coordinated successive sub-studies.

	Observation time	Experimental groups	N	Group name	Performed experiments
Study I (UAB)	120 days	Hollow chitosan nerve guide	10	hCNG-I	*Motor recovery:* electrophysiology non-invasive (60, 90, 120 days); *Sensory recovery:* von Frey algesimetry (7, 60, 90, 120 days); *Histomorphometry*
		1st generation chitosan film enhanced chitosan nerve guide	7	CFeCNG^{1st}	
Study II (ULUND)	56 days	Healthy rats: Hollow chitosan nerve guide	8	hCNG-II^{healthy}	*Analysis of regenerative matrix*: presence of axons and activated and apoptotic Schwann cells by immunhohistochemistry; *Analysis of sensory dorsal root ganglion activation* by immunohistochemistry
		Diabetic GK rats: Hollow chitosan nerve guide	8	hCNG-II^{diabetic}	
		Healthy rats: 2nd generation chitosan film enhanced chitosan nerve guide	8	CFeCNG$^{2nd\text{-}healthy}$	
		Diabetic GK rats: 2nd generation chitosan film enhanced chitosan nerve guide	8	CFeCNG$^{2nd\text{-}diabetic}$	
Study III (MHH)	120 days	Autologous nerve graft	8	ANG	*Motor recovery:* electrophysiology non-invasive (60, 90 days) and finally invasive (120 days) and Muscle weight ratio; *Sensory recovery:* von Frey algesimetry (7, 60, 90, 120 days); *Histomorphometry; Immunohistochemistry*
		Hollow chitosan nerve guide	8	hCNG-III	
		2nd generation chitosan film enhanced chitosan nerve guide	8	CFeCNG^{2nd}	
		2nd generation chitosan film enhanced chitosan nerve guide with FGF-2 overexpressing Schwann cells	8	CFeCNG^{2nd}-SC-FGF-2^{18kDa}	

only a 5 mm segment was removed providing an increased length of the distal nerve end. For nerve reconstruction using the different types of chitosan nerve guides, the liquid-soaked guides (>30 min in 0.9% NaCl solution or Schwann cell medium) had a length of 19 mm and bridged a 15 mm defect between the two nerve ends. The nerve guides were sutured with one epineurial stitch at each end (9–0, EH7981G, Ethilon, Ethicon, Scotland). For transplantation of reversed autologous nerve grafts (ANGs) no nerve tissue was removed, but the distal nerve end again transected 15 mm distal to the first transection point, flipped (proximal-distal direction) and turned 180° around its longitudinal axis before three epineurial sutures were placed with a spacing of 120° from each other.

2.4. Preparation of FGF-2 overexpressing Schwann cells for enrichment of CFeCNGs

Neonatal rat Schwann cells (neoSC) were obtained, cultured and genetically modified as described before [19,21]. Briefly, sciatic nerves were harvested from Hannover Wistar rat pups (p1-3) and neoSC isolated and purified by immunopanning until >90% pure neoSCs cultures were achieved.

Three days prior to transplantation, neoSCs (passage 8–9) were genetically modified using the nucleofection technique (Basic glial cell nucleofection kit and program T-20 of AMAXA II device, LONZA, Cologne, Germany) to introduce the non-viral plasmid encoding for FGF-2^{18kDa} (pCAGGS-FGF-2-18 kDa-Flag, NCBI GenBank accession NM_019305.2, 533–994 bp) as described before [19]. Afterwards, cells were cultured for 24 h on poly-L-lysine-coated 6 well-plates (Sigma–Aldrich, Munich, Germany) with neoSC-specific culture medium (DMEM, 1% Penicillin/streptomycin, 2 mM L-glutamine, 1 mM sodium pyruvate and 10% fetal calf serum [all PAA Laboratories, Coelbe, Germany]) to recover from transfection. On the following day, the genetically modified neoSCs were seeded on the central part of CFs within 2nd generation CFeCNGs (CFeCNG^{2nd}-SC-FGF-2^{18kDa}). Therefore, 5×10^5 cells were suspended in a volume of 30 µl culture medium and 15 µl applied on both sides of the CF. After 30 min to allow cell adhesion, the scaffolds were covered with culture medium to avoid drying of the nerve guides and incubated at 37 °C in humidified atmosphere with 5% (v/v) CO_2 for another 24 h. On the next day, the medium was changed to serum free-N2 medium and the cell-seeded nerve guides were again incubated overnight in preparation for surgery.

5×10^4 cells were seeded into 24-well plates for analyses of cell purity and transfection efficiency in corresponding sister cultures after immunostaining with SC specific α-S100 antibody 1:200 (Dako, Denmark) in phosphate buffered salt solution (PBS)/0.3% Triton-X-100/5% BSA solution or anti-Flag antibody 1:200 (all Sigma–Aldrich, Germany) and Alexa 488-labelled goat α-rabbit secondary (Invitrogen, Germany) antibody or Alexa-555-labelled goat α-mouse IgG secondary antibody 1:500 (Invitrogen, Germany), respectively [19]. All cell nuclei were counterstained with DAPI (1:1000 in PBS, Sigma–Aldrich, Germany). The transplanted cells had a purity of 90.2% S100-+ SCs and 90.1% of the cells were Flag-+ after nucleofection.

In order to proof that the neoSCs successfully adhered to the chitosan surfaces and populated the CFs within the nerve guides, sample CFeCNG^{2nd} were seeded with 5×10^5 neoSCs and kept in culture for up to 16 days. Fig. 1E–F shows representative photomicrographs taken at day 10 and day 16 in vitro, which clearly demonstrate that the cells densely populated both surfaces of the CF in the SC-typical fish-swarm like manner.

2.5. Assessment of the regenerative matrix at day 56 after surgery (study II)

At 56 days after surgery a regenerative matrix, sufficient for immunohistochemical analyses, was formed in the 15 mm long nerve defect within the nerve guides. The contents of the conduits together with the respective proximal and distal nerve ends were harvested as described before [6,15,17]. Briefly, the tube content was processed for sectioning using a cryostat and longitudinal sections at 4 µm thickness were collected on Super Frost® plus glass slides (Menzel-Gläser, Germany). On these sections, immunohistochemistry was performed to evaluate (1) presence of axons by neurofilament staining (anti-human neurofilament protein, 70 kDa NF-L [DAKO Glostrup, Denmark], 1:80 in 0.25% Triton-X 100 and 0.25% FCS in phosphate buffered salt solution [PBS]/Alexa Fluor 594 conjugated goat anti-mouse IgG [Invitrogen, Molecular Probes,

USA], diluted in 1:500 in PBS), and (2) activated Schwann cells and apoptotic Schwann cells, respectively, by anti-activating transcription factor 3 (ATF3) and anti-cleaved caspase 3 staining (rabbit anti-ATF-3 polyclonal antibody [1:200; Santa Cruz Biotechnology, USA] or anti-cleaved caspase-3 antibody [1:200; *Invitro* Sweden AB, Stockholm, Sweden]; both diluted in 0.25% Triton-X 100 and 0.25% FCS in PBS/Alexa Fluor 488 conjugated goat anti-rabbit IgG [Invitrogen, Molecular Probes, USA], diluted in 1:500 in PBS). The Schwann cells were identified on their location and the oval shaped nuclei [6,22]. Furthermore, double staining for ATF3 or cleaved caspase 3 and S-100 was additionally performed as earlier described and mounted in Vectashield® (Vector Laboratories, Inc. Burlingame, USA) [17,22]. Finally, the slides were mounted with 4′,6′-diamino-2-phenylindole DAPI to visualize the nuclei (i.e. for counting the total number of the cells) and cover slipped.

For analysis, as earlier described [6,15,17], blind-coded sections were digitized and the presence of outgrowing axons in the formed matrix inside the conduits was evaluated (i.e. present or non-present) in three randomly selected sections at two different locations: in the center of the formed matrix as well as in the distal nerve segment just distal to the distal suture line. The stained cells for cleaved caspase-3 and ATF-3 were also counted in three sections (image size 500 × 400 μm; mean of the three sections calculated for each rat) at two different levels in the matrix and in the adjacent sciatic nerve: at 3 mm distal to the proximal nerve suture, in the center of the formed matrix in the nerve guides and in the distal segment (see above). The same squares were also used for counting the total number of DAPI stained cells (no/mm^2). The images (20× magnification) were analyzed with NIS elements (Nikon, Japan).

2.6. Assessment of sensory dorsal root ganglia at day 56 after surgery (study II)

At the same time as the content of the nerve guides was harvested, the dorsal root ganglia (DRG) L4 and L5 were collected bilaterally and processed for cryostat sectioning. Longitudinal sections (8 μm thickness) were collected on Super Frost® plus glass slides (Menzel-Gläser, Germany) for evaluation of cell activation (i.e. ATF3) and presence of the neuroprotective substance Heat Shock Protein 27 (HSP27; [6,23]). The DRG sections were air dried, washed in PBS for 15 min, and thereafter incubated for ATF-3 immunohistochemistry as described above or incubated with a primary goat-anti-HSP27 antibody [sc-1048, Santa Cruiz Biotechnology, USA; dilution 1:200 in 0.25% Triton-X-100 (Sigma–Aldrich, USA) and 0.25% bovine serum albumin (BSA; Sigma–Aldrich, USA) in PBS overnight at 4 °C. The anti-HSP27 antibody was detected with the secondary Alexa flour 488 donkey anti-goat antibody (Molecular Probes, Eugene, Oregon, USA; dilution 1:500) in PBS for 2 h at room temperature followed by a further wash with PBS for 3 × 5 min. Finally, theses sections were cover-slipped with Vectashield® (Vector Laboratories, CA, USA) containing DAPI for counterstaining of the nuclei. Three sections from each DRG were analyzed for ATF3 and HSP27 staining, respectively, and mean values were calculated from each rat.

To analyze the presence of ATF3 activated sensory neurons and the expression of HSP27 in the DRGs, images were captured at 10× magnification with the same equipment and processed as above followed by import into Image J. ATF3 stained sensory neurons were quantified as described [24] and expressed as percent of total number of sensory neurons (i.e. DAPI stained cells). A region of interest (ROI) covering 75x75 pixels was determined to analyze HSP27 expression. The tool threshold was used to determine the immunolabelling with the intensity threshold decided by adding three times the standard deviation of the background to the mean intensity ($\bar{x} + 3 \times$ SD). Measurement of the immunostained area was performed across the entire section and expressed in percent of the total area of the section; thus, both intensity of neurons and their satellite cells were included. Furthermore, the HSP27 expression was also expressed as a ratio; i.e. percent HSP27 at the experimental side divided by the expression on the control side.

2.7. Assessment of functional motor and sensory recovery

2.7.1. Motor recovery: electrophysiological tests

The tests were performed according to previous description [15,18]. Briefly, the animals were anesthetized and monopolar needle stimulation electrodes were transcutaneously placed at the sciatic notch. Single electrical impulses (100 μs duration, supramaximal intensity) were applied and the compound muscle action potentials (CMAPs) were recorded from the tibialis anterior muscle (TA) and the plantar interosseus muscles (PL). The active recording electrode was located in the respective muscle belly, the reference electrode in the second or fourth toe and the ground needle electrode was inserted in the skin at the knee. To ensure a steady body temperature the animals were placed in a prone position on a thermostatic blanket. For invasive recordings (final examination in study III), the sciatic nerves were exposed consecutively on the lesioned and non-lesioned side and stimulated proximal to the lesion site using a bipolar steel hook electrode (single electrical pulses, 100 μs duration, supramaximal, but not exceeding 8 mA). Recording sites remained as described above. The CMAPs were recorded and displayed in an EMG apparatus (Sapphyre 4ME, Vickers Healthcare Co, United Kingdom, at UAB (study I) or Keypoint Portable, Medtronic Functional Diagnostics A/S, Denmark, at MHH (study III)).

Evaluation parameters included the latency of the arriving signals and the amplitude ratio (amplitude [mV] recorded from lesioned side divided by non-lesioned side values). For latency evaluation all values obtained from animals showing distal muscle reinnervation were taken into account for statistical tests. If no evoked CMAP was detected a 0.00 value was noted and included for statistical analysis in case of the amplitude ratio.

2.7.2. Sensory recovery: mechanical pain threshold assessment (von Frey algesimetry)

Sensory recovery was determined via von Frey test as previously described [18,19,25]. In brief, animals were placed into plastic compartments located on a metallic mesh grid 15–30 min before starting the experimental session for habituation. Then, the probe of a von Frey algesimeter (UAB (study I): Bioseb, Chaville, France; MHH (study III): IITC Inc, Life Science, USA) was applied for stimulation of the lateral paw area innervated by the tibial and sural nerve branches of the sciatic nerve. The stimulation force required to elicit a withdrawal response from the animals was noted in grams [g] and three measurements per stimulation site were used to determine a mean value. A cut-off force was set to 40 g, when either no withdrawal was observed or no active response occurred. To minimize variations between days, the values are stated in % compared to data obtained from the non-lesioned, healthy side calculated by the following formula: lesioned side [g]/non-lesioned side [g] *100.

In Study I the test was performed 7 days, 21 days, 30 days, 60 days, 90 days, and 120 days after nerve guide implantation. Subsequently, the saphenous nerve was cut and the test was conducted once more on day 122. In Study III the test was performed 7 days, 60 days, 90 days, and 120 days after nerve reconstruction.

For statistical analysis all measured values were used and in case of no response the cut-off force was included. In the course of Study I successful recordings from the PL muscle positively correlated with withdrawal responses seen in von Frey test only after deletion

of the saphenous nerve function on day 122. This additional surgery was avoided in Study III and only values obtained from animals showing PL CMAPs were used for final calculation of sensory recovery level, while cut-off forces (40 g) were included for animals that did not show CMAP.

2.8. Nerve immunohistochemistry and morphometry

2.8.1. Nerve immunohistochemistry

After completion of the final functional tests, animals were sacrificed and the regenerated nerve tissues with the surrounding chitosan nerve guides were harvested for further analysis. In study I the complete nerve guide was removed from the regenerated nerve tissue and the macroscopic appearance assessed. In study III, the entire samples (nerve tissue together with nerve guides) were fixed in 4% PFA overnight (4 °C) for subsequent paraffin-embedding and (immuno-) histological analysis. Serial 7 μm sections were obtained (two series of 20 blind-coded sections each, one in the region without CF and one with CF, each covering a distance of about 630 μm). Sample sections were processed for hematoxylin eosin (HE) and trichrome (collagen) staining in order to visualize the tissue within the nerve guides. For the trichrome-staining, sections were subjected to hematoxylin (Roth, Germany), before being washed-offed under tap water. Afterwards the slides were incubated in 20 ml staining solution containing acetic acid (1 ml in 99 mlH_2O, Merck, Germany) and acetic fuchsin (0.5 g, in 100 ml 1% acetic acid, Merck, Germany) mixed with 10 ml light green (1 g in 100 ml 1% acetic acid, Chroma Gesellschaft, Schmidt & Co., Germany) and 10 ml wolframate phosphoric acid (1 g in 100 ml H_2O, Merck, Germany). Following a washing step in distilled water, the slides were subjected to 1% acetic acid, before being pressed with filter paper, dehydrated, and mounted with corbit-balsam (Hecht, Germany).

Immunohistology was performed on sections consecutive to the ones processed for HE or trichrome staining by double-staining for neurofilament and choline acetyltransferase (ChAT). Therefore, the sections were incubated in 5% horse serum in PBS for blocking before incubation with primary goat α-ChAT antibody (1:50, in blocking solution, AB144P, Millipore, Germany) at 4 °C overnight. Following three washing steps in PBS, incubation with Alexa 555-conjugated secondary donkey α-goat antibody (1:500, in blocking solution, A21422, Invitrogen, Germany) for 1 h at RT was performed and succeeded by another washing round. After a second blocking step (3% milk powder/0.5% triton X-100 in PBS) overnight incubation with primary rabbit α-NF200 antibody (against phosphorylated NF–H, 1:500, in blocking solution, N4142, Sigma–Aldrich, Germany) was conducted. Three washing steps followed, before incubation with Alexa 488-conjugated secondary goat α-rabbit antibody (1:1000, in blocking solution, A11034, Invitrogen, Germany) for 1 h at RT and counterstaining with DAPI (1:2000, in PBS, Sigma–Aldrich, Germany) was performed. Finally, sections were mounted using Mowiol (Calbiochem, Germany).

For qualitative analysis, representative photomicrographs of HE and trichrome stained sections were taken with the help of BX53 and BX51 microscopes and the programs CellSense Dimension and CellSense Entry (all Olympus, Germany). Immunohistochemistry images were digitized with the help of a fluorescence microscope (BX60, Olympus, Germany) and cellP software (Olympus, Germany).

2.8.2. Nerve morphometry

Together with the harvest of the regenerated nerve tissue and nerve conduits for nerve histology, distal nerve segments (5 mm segments from distal nerve guide end into distal direction) were harvested and processed as described before [15,18]. In short, the tissue was subjected to an initial fixation based on glutaraldehyde containing fixatives and post-fixed in 1% OsO_4. Following dehydration samples were processed for epoxy resin embedding and semi-thin (2.5 μm) transverse sections were cut in proximal direction using an Ultracut UCT ultramicrotome (Leica Microsystems, Germany) and stained with toluidine blue. Finally, total myelinated fiber number, cross sectional area, nerve fiber density, axon diameter, fiber diameter, g-ratio, and myelin thickness were determined for all experimental groups of study I and study III in addition to values obtained from healthy control samples. All histomorphometry was performed at the University of Turin (UNITO, Italy) with the help of systematic random sampling as described before [15].

2.9. Muscle weight ratio

Upon harvest of the nerve tissue samples also the tibialis anterior and gastrocnemius muscles were explanted from study III animals. The fresh muscle weight from the ipsilateral lesioned side was then compared to the weight measured from contralateral healthy muscles to calculate the muscle weight ratio ([g] ipsilateral/[g] contralateral). The ratios from all animals were included into statistical analysis irrespectively of the electrodiagnostic or macroscopic outcome of the nerve regeneration process.

2.10. Statistics

The data obtained in the different experimental settings were subjected to statistical analysis using Kruskal–Wallis test or two-way ANOVA (Analysis of Variance) followed by Dunn's or Tukey's multiple comparison test or by Mann–Whitney U-test (with subsequent Fisher's test; [6]) as specifically indicated in the results section. Differences concerning expression of HSP27 in DRGs on the control and experimental sides were examined with the Wilcoxon signed rank test. The proportion of animals per group that displayed a predefined qualitative parameter (evoked CMAP) was calculated as percentage (0–100%) and analyzed with the Chi-Square-Test. The p-value was set at < 0.05 as level of significance. For statistical analysis either the statistical package SPSS (version 17.0 or 20.0, IBM, USA) or GraphPad InStat software, version 5.0.3.0 & 6.00 (Graphpad Software, CA, USA) were used.

3. Results

In the first part of the results section long term study results obtained from Study I and Study III will be presented. In both studies, examination of motor and sensory functional recovery and histo-morphometry were performed over a period of 120 days after reconstruction of 15 mm rat sciatic nerve defects. In the second part of the results section short term results obtained from Study II will be presented. Here, the regenerative matrix formed after nerve guide grafting and the activation of sensory DRG neurons were immunohistologically analyzed 56 days after reconstruction of 15 mm rat sciatic nerve defects in healthy and diabetic rats. Diabetic Goto-Kakizaki rats could not be subjected to long-term studies because of their expected limited life-span and ethical approval.

3.1. Long term evaluation of the effects of different reconstruction approaches on functional recovery and axonal regeneration

The long term evaluations were performed to elucidate the potential of chitosan film enhanced chitosan nerve guides of the first ($CFeCNG^{1st}$, continuous chitosan film, study I) and second ($CFeCNG^{2nd}$, chitosan film with holes, study III) generation to support peripheral nerve regeneration across critical length defects. In an additional experimental group, $CFeCNG^{2nd}$ were enriched with

FGF-2^{18kDa} overexpressing Schwann cells (CFeCNG^{2nd}-SC-FGF-2^{18kDa}). Control animals received either nerve reconstruction with hollow chitosan nerve guides (hCNG-I or hCNG-III, respectively) or with autologous nerve grafts (ANG).

3.1.1. Electrophysiological assessment

The qualitative results are summarized in Table 2. Non-invasive electrophysiological recordings did not detect evoked CMAPs before day 60 after nerve repair.

At this time point, regenerating fibers had reached the TA muscle in 3 out of 10 hCNG-I animals and in 2 out of 7 CFeCNG^{1st} animals in study I. At the same examination time point in study III, reinnervation of the TA muscle did already occur in 7 out of 8 ANG animals and in none of the other experimental groups. Recordings from the more distal PL muscle in study I also detected reinnervation in the same 3 hCNG-I animals but only in one of the TA-positive CFeCNG^{1st} animals. In study III, PL muscle reinnervation was already detectable in 7 out of 7 examinable ANG animals (one drop out due to events of autotomy), but not in the other groups.

Upon the next examination at day 90 after nerve reconstruction, additional 1 or 2 animals, respectively, displayed reinnervation of the TA muscle in study I (Table 2), increasing the percentage of animals with muscle reinnervation to 40% in hCNG-I group and 57% in CFeCNG^{1st} group. In study III (Table 2), 100% of ANG animals displayed TA muscle reinnervation and a gain of motor function was detectable in hCNG-II animals while CFeCNG^{2nd} caught up with the CFeCNG^{1st} animals. In contrast, the number of animals with detectable reinnervation of PL muscles did not increase in study I in the hCNG-I group, but a higher percentage of animals demonstrated motor recovery in the CFeCNG^{1st} group. In study III, PL muscle reinnervation was started in nerve guide repaired groups, displaying a slightly better result in the CFeCNG^{2nd} group than in the hCNG-III group.

At the final examination 120 days after nerve reconstruction (Table 2), TA and PL CMAPs increased in amplitude but muscle reinnervation was not found in further animals in study I. In contrast, TA muscle reinnervation was detected, in final invasive testing, in an increased number of study III animals of the CFeCNG^{2nd} as well as the CFeCNG^{2nd}-SC-FGF-2^{18kDa} group. Reinnervation of PL muscle was detectable in one additional animal of the CFeCNG^{2nd} group.

When comparing the performance of CFeCNG^{1st} and CFeCNG^{2nd}, while at 60 days after nerve repair CFeCNG^{1st} performed better than CFeCNG^{2nd}, at 120 days CFeCNG^{2nd} supported functional motor recovery in a higher percentage of animals. Additional enrichment of the CFeCNG^{2nd} with FGF-2^{18kDa} overexpressing Schwann cells did not allow for the level of distal target reinnervation displayed in the hCNG and CFeCNG groups.

Quantitative results were calculated for the latencies and amplitude ratios of the recorded CMAPs at day 120 after nerve reconstruction and no significant differences between the groups were detected in study I (non-invasive measurements, mean ± SEM): TA muscle latency hCNG-I = 4.50 ± 0.82 ms; CFeCNG^{1st} = 4.05 ± 0.17 ms; TA muscle amplitude ratio hCNG-I = 16.52 ± 8.10%; CFeCNG^{1st} = 24.80 ± 10.41%; PL muscle latency hCNG-I = 5.19 ± 0.16 ms; CFeCNG^{1st} = 5.43 ± 0.36 ms; PL muscle amplitude ratio hCNG-I = 12.86 ± 7.87%; CFeCNG^{1st} = 7.75 ± 4.55%. Fig. 2 summarizes the quantitative results obtained from study III at day 120 after nerve reconstruction (invasive measurements). Latencies (Fig. 2A) were significantly increased in comparison to healthy nerve values in the CFeCNG^{2nd} and CFeCNG^{2nd}-SC-FGF-2^{18kDa} groups when CAMPs were recorded from the TA muscle. This was also the case for all groups, including ANG and hCNG-III, when CAMPs were recorded from the PL muscle. TA CMAP amplitude ratios (Fig. 2B) were decreased in comparison to ANG values in all nerve guide groups but this difference was significant only for the hCNG-III and the CFeCNG^{2nd}-SC-FGF-2^{18kDa} groups. Due to high variance, PL CMAP amplitude ratios were significantly lower in comparison to ANG values only in the CFeCNG^{2nd}-SC-FGF-2^{18kDa} group (Fig. 2B). These quantitative results indicate that not only muscle reinnervation in general but also the amount of recruited regenerated fibers in the CFeCNG^{2nd} group approximated that in the ANG group.

3.1.2. Muscle weight ratio

As an additional indicator for motor recovery, the hindlimb TA and gastrocnemius (GA) muscles wet weight ratios were determined in study III. As depicted in Fig. 2C, statistical analysis revealed again that CFeCNG^{2nd} and ANG group values were not significantly different from each other, although ANG group had the highest ratios. Significantly lower muscle weight ratios compared to ANG group values were detected for the TA muscle and the GA muscle in the CFeCNG^{2nd}-SC-FGF-2^{18kDa}group, and for the GA muscle additionally in the hCNG-III group. These results underscore the relatively good performance of the CFeCNG^{2nd} already detected in the electrophysiological tests.

Table 2
Overview of the gain in electrophysiologically detectable motor recovery (evocable compound muscle action potentials) during the observation in sub study I and sub study III. Significant differences ($p < 0.05$) are indicated as follows: + versus ANG,# hCNG-I versus CFeCNG^{1st},§ versus CFeCNG^{2nd}, $ versus CFeCNG^{2nd}-SC-FGF-2^{18kDa},* CFeCNG^{1st} versus CFeCNG^{2nd}.

		60 days			90 days			120 days		
		Animals/ group	Percentage	Significant difference	Animals/ group	Percentage	Significant difference	Animals/ group	Percentage	Significant difference
Tibialis anterior muscle										
Study I	hCNG-I	3/10	33%	+	4/10	40%	+	4/10	40%	+
	CFeCNG^{1st}	2/7	29%	+	4/7	58%	+#	4/7	58%	+#
Study III	ANG	7/8	88%		8/8	100%		8/8	100%	
	hCNG-III	0/8	0%	+	2/7	29%	+§ $	3/7	43%	+§ $
	CFeCNG^{2nd}	0/8	0%	+*	4/7	58%	+	6/7	86%	+*
	CFeCNG^{2nd}-SC-FGF-2^{18kDa}	0/8	0%	+	0/8	0%	+§	5/7	71%	+§
Plantar muscle										
Study I	hCNG-I	3/10	33%	+	3/10	33%	+	3/10	33%	+
	CFeCNG^{1st}	1/7	14%	+	3/7	43%	+	3/7	43%	+
Study III	ANG	7/7	100%		7/7	100%		7/7	100%	
	hCNG-III	0/8	0%	+	3/7	43%	+ $	3/7	43%	+§ $
	CFeCNG^{2nd}	0/7	0%	+*	3/6	50%	+	4/6	67%	+*
	CFeCNG^{2nd}-SC-FGF-2^{18kDa}	0/6	0%	+	1/6	17%	+§	1/6	17%	+§

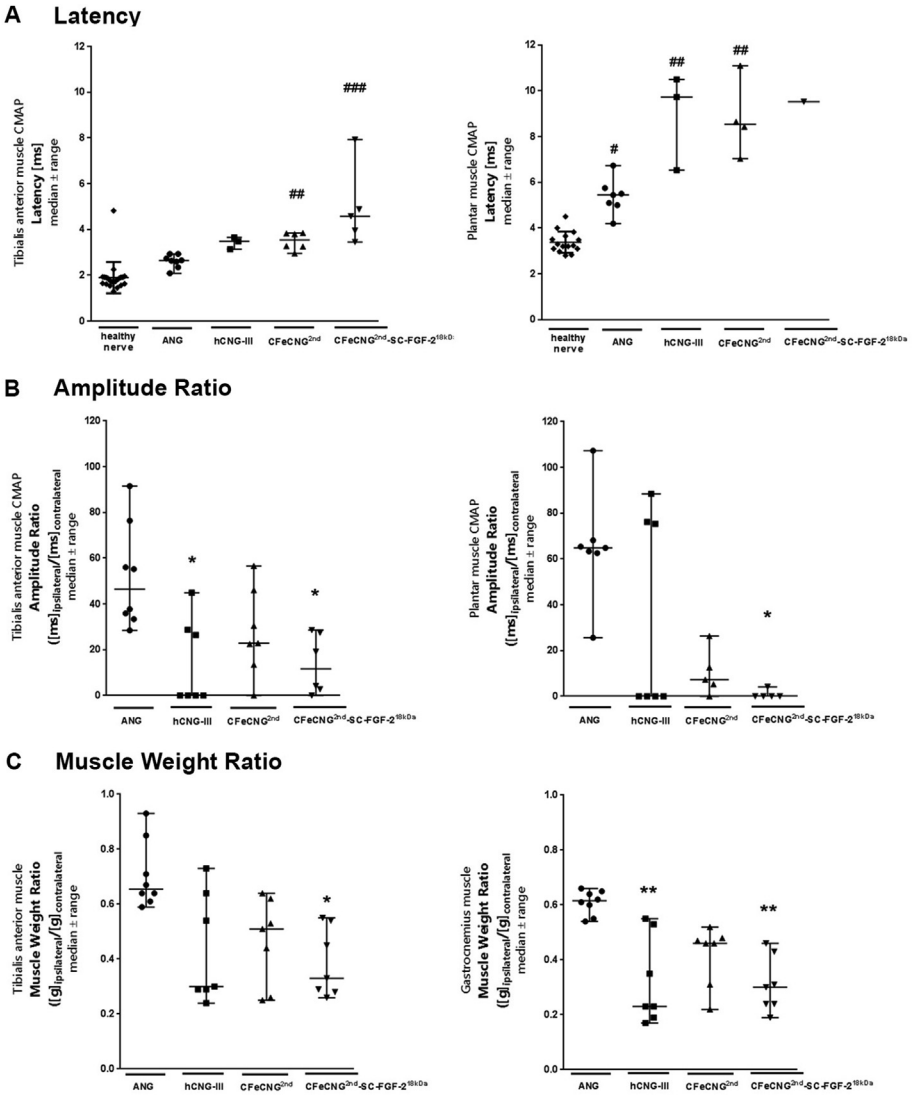

Fig. 2. Dot plot depicting the latency (A) and amplitude ratio (B) of compound muscle action potentials (CMAPs) recorded during final electrophysiological tests performed 120 days after nerve surgery in the tibialis anterior muscle (left column) and plantar muscles (right column). (C) Dot plot depicting tibialis anterior muscle (left column) and gastrocnemius muscle (right column) muscle weight ratios calculated after final electrophysiological measurements. Results were tested for significance ($p < 0.05$) by Kruskal–Wallis test, followed by Dunn's multiple comparison. #$p < 0.05$, ##$p < 0.01$, ###$p < 0.001$ vs healthy control values; *$p < 0.05$, **$p < 0.01$ vs ANG group.

3.1.3. Von Frey algesimetry

The results obtained for evaluation of sensory recovery using the von Frey test are summarized in Fig. 3. The withdrawal response obtained at the healthy contralateral paw was calculated as 100%. From the injured/regenerating paw two types of withdrawal response have been recorded, a response at lower force compared to the contralateral paw (<100%, higher or maladaptive mechanosensitivity than normal) or a response at higher force compared to the contralateral paw (>100%, less mechanosensitivity than normal).

Study I (Fig. 3A) revealed no withdrawal responses within the first 21 days following sciatic nerve transection indicating complete denervation of the animals plantar surface. However, after 30 days, some animals of both groups (hCNG-I and CFeCNG^{1st}) demonstrated a withdrawal of the lesioned paw at lower stimulus intensities than seen for the contralateral, intact side. At 60 days after nerve reconstruction, 7 out of 10 animals from the hCNG-I group and all animals of the CFeCNG^{1st} displayed withdrawal responses at low stimulus intensities. During the next examination at 90 days and 120 days after nerve reconstruction, all animals regardless of the received treatment responded to the stimulation at low stimulation intensities. To exclude false positive responses due to sprouting events from branches of the saphenous nerve [25], this nerve was then cut and the von Frey test conducted once more on day 122. At this time point, 4 out of 10 animals (40%) in the hCNG-I group showed withdrawal responses, resulting in 103 ± 6.57% response compared to contralateral, and 3 out of 7 animals (43%) demonstrated a withdrawal response in the CFeCNG^{1st} group, resulting 117 ± 8.20% response compared to contralateral. These latter results indicate that the withdrawal responses in previous test days were in part due to hypersensitivity caused by collateral spouting of the saphenous nerve and not fully attributable to sciatic nerve regeneration.

Study III (Fig. 3B) also revealed a gain in mechanosensitivitiy over time after nerve reconstruction. At 60 days the following numbers of animals withdrew their paws following lower stimulation intensities than recorded for the contralateral, healthy side: ANG group: 6 out of 7, hCNG-III group: 4 out of 7, CFeCNG^{2nd} group: 3 out of 6, and none in the other groups. In the course of the study, additional animals responded to the stimulation. To avoid an

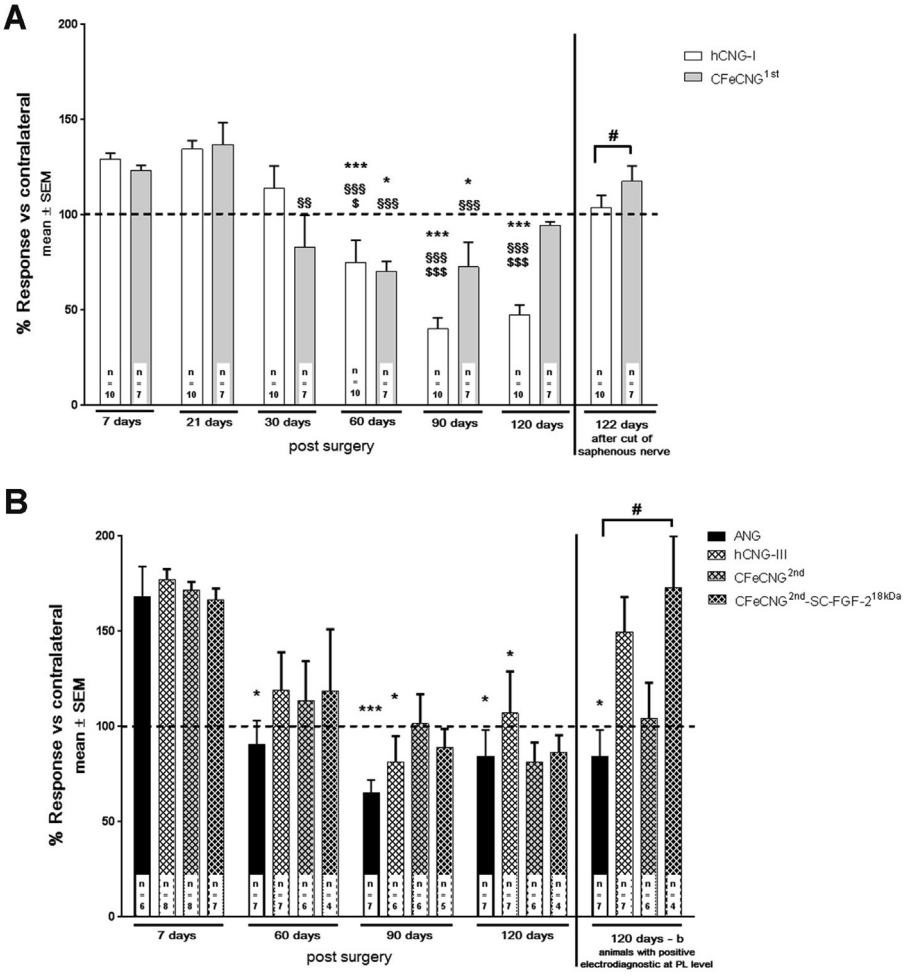

Fig. 3. Results of mechanical pain threshold assessment in the course of Study I and Study III expressed as percentage of values obtained from the contralateral, non-lesioned side. (A) Results obtained during Study I at various time points. Following 120 days of observation, the saphenous nerve was cut to exclude false positive responses due to saphenous nerve collateral reinnervation. This resulted in a withdrawal response only from animals that also displayed reinnervation of PL muscles in electrophysiological tests. Results of the final mechanical pain threshold evaluation are depicted in the last pair of columns (122 days). (B) Results obtained during Study III. The last set of columns (120 days-b) depicts the calculation corrected according to electrodiagnostic results at the PL muscle level (determined values included for animals with positive CMAP and cut-off values included for animals without recordable CMAP). Variations in animal numbers are due to exclusions because of autotomy events. Significant differences ($p < 0.05$) were determined by Two-Way ANOVA, followed by Tukey's multiple comparisons tests. #$p < 0.05$; *$p < 0.05$, **$p < 0.01$, ***$p < 0.001$ vs 7 day results within same group; §§$p < 0.01$, §§§$p < 0.001$ vs 21 day results within same group; $ $p < 0.05$, $$$ $p < 0.001$ vs 30 day results within same group.

additional surgery (cutting of the saphenous nerve), only values from animals that showed recordable CMAPs at the PL muscle during final electrophysiological tests were accepted for the 120 days-b calculation (Fig. 3B last set of columns), while the cut-off force (40 g, see Section 2.7.2) was included for animals demonstrating no reinnervation of the PL muscle. Thereby, no significant differences were detected between the ANG group (84.40 ± 13.70% response compared to contralateral) and the hCNG-III (149.50 ± 18.52%) or CFeCNG^{2nd} (104.04 ± 18.87%) groups. The CFeCNG^{2nd}-SC-FGF-2^{18kDa} group (172.90 ± 26.99%) did not display successful sensory recovery. Overall the values indicate that recovery of the mechanosensitivity approximated normal values most closely in the CFeCNG^{2nd} group.

3.1.4. Macroscopic inspection upon explantation

Prior to nerve tissue harvest for histomorphometrical evaluation, macroscopic observation of the reconstructed nerves in study I visualized in the hCNG-I group a nerve cable bridging the 15 mm gap in 5 out of 10 (50%) animals (Fig. 4A). In the CFeCNG^{1st} group, the bridging tissue was split into two cables and visible in 5 out of 7 (71%) animals (Fig. 4B). The two regenerated tissue cables were separated from each other closely proximal to the central CF and fused again distal to it (Fig. 4B).

In study III all animals of the ANG group showed bridged nerve ends. Nerve guide repair resulted in the following macroscopically visible tissue regeneration outcome: hCNG-III group single tissue cables in 4 out of 7 seven animals (57%); CFeCNG^{2nd} group: two tissue cables, one in each compartment of the nerve guide, in 7 out of 7 (100%) animals; CFeCNG^{2nd}-SC-FGF-2^{18kDa} group: two tissue cables, one in each compartment of the nerve guide, in 6 out of 7 animals plus a single cable (in one compartment only) in the last animal.

The macroscopic inspection demonstrated that nerve regeneration through chitosan guides was increased by introducing into these guides continuous chitosan films (CFeCNG^{1st}) and further improved by the perforated chitosan films (CFeCNG^{2nd}), while additional enrichment with FGF-2^{18kDa} overexpressing Schwann cells (CFeCNG^{2nd}-SC-FGF-2^{18kDa}) did not provide a synergistic effect.

3.1.5. Nerve histology

To reveal differences in regenerated tissue organization in study

III, histological cross-sections were prepared from whole nerve guide/nerve tissue samples at mid-graft level (with visible CF in the respective groups) and at ~1 mm proximal to the distal suture side (without CF in the respective groups). As shown in Fig. 5, the two regenerated tissue cables in the CFeCNG^{2nd} and CFeCNG^{2nd}-SC-FGF-2^{18kDa} groups appeared to be connected to each other through the holes inside the CF. In some cases also small vessels traveling through the holes were visible with the help of the microsurgical microscope (Fig. 5A–B). Single histological cross-sections taken from the mid-graft level and stained for collagen (trichrome staining) also displayed these connections (Fig. 5C–F), although the staining procedures partly caused the dissolution of CF out of the sections. Interestingly, no axons traveling with these tissue bridges could be detected in neurofilament staining (see below).

Fig. 6 shows representative photomicrographs of HE stained sections from the ANG group (Fig. 6A–B) or of a regenerated nerve inside hCNG-III grafts (Fig. 6C–D). Fig. 6E–F demonstrates that two tissue cables, which were separated by the z-shaped CF regenerated in CFeCNG^{2nd} grafts (Fig. 6E) and fused again prior to reconnecting to the distal nerve end (Fig. 6F).

Furthermore, consecutive sections were double-stained for NF200-neurofilament and ChAT to demonstrate the presence of motor fibers within the regenerated nerve cables. Fig. 7 shows representative photomicrographs from the ANG group (Fig. 7A–C), the hCNG-III group (Fig. 7D–F), and the CFeCNG^{2nd} group (Fig. 7G–H).

3.1.6. Nerve morphometry

Fig. 8 depicts the results of the stereological assessment of the regenerated myelinated axons in a segment 5 mm distal to the nerve grafts. The total numbers of myelinated fibers (Fig. 8A) are significantly different in the ANG group compared to the healthy nerve, but no differences are detectable between the experimental groups.

With regard to axon and fiber diameters and myelin thickness (Fig. 8B), single significant differences from healthy nerve values could be detected, but again no differences are detectable among the experimental groups.

These results indicate that once regeneration occurred through any of the used graft types, axonal regeneration at a short distance from the graft or guide (in contrast to functional recovery of more distal targets) follows a similar course in all the reconstruction conditions assayed.

3.2. Short term evaluation of the regenerative matrix and dorsal root ganglia

The pre- and postoperative (at 56 days post surgery) blood glucose levels in the healthy and diabetic GK rats were measured and are presented in Table 3, with significantly higher values in the diabetic GK rats. Furthermore it can be revisited in Table 3 that in contrast to other diabetic animal models these rats developed a moderate and therefore clinically relevant increase of blood glucose levels resembling type 2 diabetes in human patients.

3.2.1. Regenerative matrix and distal nerve segment

In single animals we examined the regenerative matrices formed at earlier time points before 56 days post surgery and found that then those were not developed enough to allow comprehensive histological analyses (results not shown).

Table 4 summarizes the qualitative and quantitative data as well as the statistical correlations. At 56 days post surgery, macroscopically, a regenerative matrix was formed completely extending between the proximal and distal nerve stumps in 6 of 8 animals (75%) in the hCNG-II^{healthy} group and in 4 of 8 animals (50%) in the hCNG-II^{diabetic} group. In groups where CFeCNG^{2nd} had been implanted, a complete (i.e. connecting the proximal and distal nerve segments) matrix was formed in 8/8 animals (100%) of both the CFeCNG$^{2nd\text{-}healthy}$ and the CFeCNG$^{2nd\text{-}diabetic}$ groups. In these animals, 6 of 8 (75%) of the CFeCNG$^{2nd\text{-}healthy}$ and 7 of 8 (88%) CFeCNG$^{2nd\text{-}diabetic}$ showed a matrix composed of two cables, extending on each side of the chitosan film, instead of one single cable as in the hCNG-II samples. Notably, in the CFeCNG^{2nd} guides, especially in the GK diabetic rats neovascularisation inside and outside the nerve guides was macroscopically observed.

3.2.1.1. Axonal outgrowth (neurofilament staining). The presence of axons in the formed matrices was evaluated by neurofilament staining (Fig. 9). Due to the thin matrix the exact length of axonal outgrowth was not possible to calculate as previously described [17]. Axons were present in the center of the formed matrices in 6/8 (75%) of hCNG-II^{healthy}and hCNG-II^{diabetic} rats (i.e. axons were also present in two of the incomplete matrices in the diabetic GK rats; Table 4). In all rats, where CFeCNG^{2nd} had been implanted, axons (i.e. 8/8 CFeCNG$^{2nd\text{-}healthy}$ and CFeCNG$^{2nd\text{-}diabetic}$ rats; i.e. 100%) were observed in the center of the matrix (Table 4; Fig. 9). The Chi-squared test did not reveal any differences in presence of neurofilaments in the nerve guide among the groups ($p = 0.21$; Table 4).

Neurofilament staining of the nerve segment distal to the nerve guides revealed axons in 3/8 (38%) hCNG-II^{healthy} rats and in 4/8 (50%) hCNG-II^{diabetic} rats, while all rats (100%) in which CFeCNG^{2nd} had been implanted exhibited axons in the segment just distal to the nerve guides (Table 4), irrespective of the healthy or diabetic condition. Thus, the chi-squared test showed a statistical significant difference in presence of neurofilaments in the distal nerve segment between the groups ($p = 0.005$), with differences observed between reconstructions using the hCNG-II and the CFeCNG^{2nd} ($p = 0.01$; Fisher's method; Table 4), but with no differences between healthy and diabetic rats.

3.2.1.2. Activated Schwann cells (ATF3-staining). The percentage of ATF3 stained Schwann cells was evaluated at three locations: 3 mm from the proximal suture line, at the center of the matrix formed in the nerve guide and at the distal nerve segment just distal to the nerve guide [17]. Double staining with S-100 has revealed that the evaluated cells were Schwann cells [6,17]. In general, few ATF3

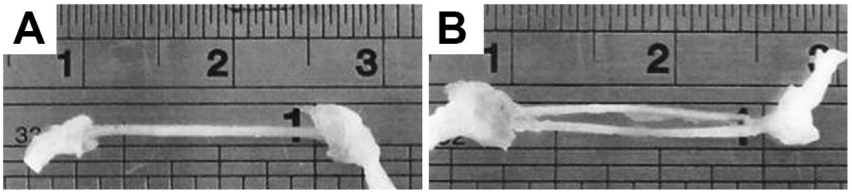

Fig. 4. Harvested regenerated nerve cable 4 months after nerve reconstruction with hollow (hCNG-I) or 1st generation chitosan film enhanced chitosan nerve guides (CFeCNG^{1st}). (A) A single nerve cable bridging the gap was seen when a hCNG-I had been used for nerve reconstruction, while (B) two bridging tissue cables (one in each compartment) were found after implantation of CFeCNG^{1st}.

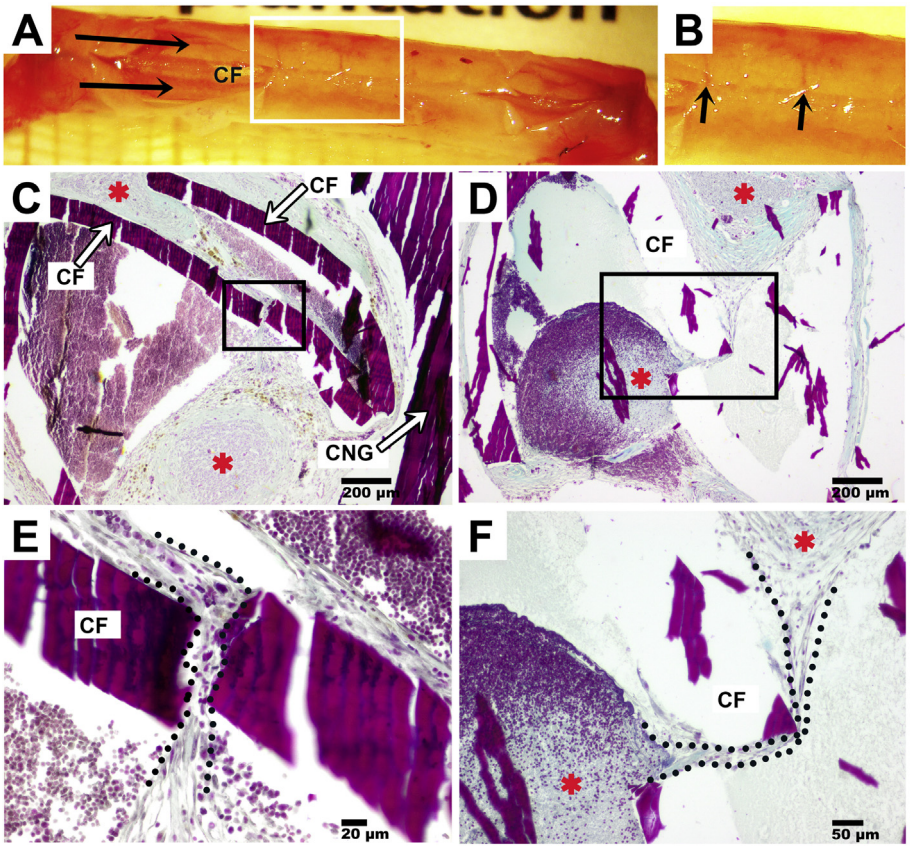

Fig. 5. (A) Photograph showing an explanted nerve guide from the CFeCNG^{2nd} group. The nerve guide is surrounded by a thin layer of connective tissue and a window has been cut to visualize two regenerated vascularized tissue cables (black arrows) separated by the chitosan film (CF). (B) The magnification of the white insert drawn in (A), clearly demonstrates the tissue growth (connective tissue and small vessels, black arrows) through the holes in the CF connecting the two regenerated tissue cables. (C, D) Sections subjected to trichrome-staining (light green) visualizing collagen. Red asterisks mark the regenerated tissue cables that are connected through the holes in the CF. The black inserts have been further magnified in (E) and (F), respectively. (E) Magnification from insert in (C), the dotted line outlines the tissue bridge between the regenerated cables. (F) Magnification from insert in (D), the dotted line outlines the tissue bridge between the regenerated cables (marked with red asterisks). CNG: chitosan nerve guide.

stained Schwann cells were observed (Fig. 10), but with differences detected between the groups (Table 4) at the three sites. There was a higher percentage of stained cells in the CFeCNG^{2nd} than in the hCNG-II samples as well as in the distal nerve segment. Furthermore, there was also higher percentage of stained cells in diabetic GK rats, except at 3 mm from the proximal suture line.

3.2.1.3. Apoptotic Schwann cells (cleaved caspase 3- staining). The percentage of cleaved caspase 3 stained Schwann cells (double staining with S-100; [17]) was evaluated at the same locations as for the ATF3 labeling (Table 4; Fig. 10) and showed differences between the groups at all the locations (Kruskal–Wallis $p = 0.0001$; 0.0001; 0.0001, respectively). At 3 mm in the matrix formed in the nerve guides, there was higher percentage of stained Schwann cells in the CFeCNG^{2nd} samples and higher percentage also in the diabetic GK rats (Table 4). At the center of the nerve guides there were no differences between hCNG-II and CFeCNG^{2nd} samples, although the diabetic GK rats exhibited a higher percentage of apoptotic Schwann cells. In contrast, the percentages in the distal nerve segment were lower in the CFeCNG^{2nd} groups as well as lower in the diabetic GK rats (Table 4; Fisher's test values).

3.2.1.4. Total number of cells (DAPI-staining). The total number of DAPI labeled cells was also assessed at the three mentioned locations and showed differences only inside the nerve guides. The number of DAPI stained cells (i.e. total number of cells) inside the nerve guides was generally higher in CFeCNG^{2nd} samples as well as higher in diabetic GK than in healthy rats. No differences between groups were observed, however, in the distal nerve segment.

3.2.2. Dorsal root ganglia (L4, L5)

Table 5 summarizes the quantitative data as well as the statistical analyses.

3.2.2.1. Activated sensory neurons (ATF3-staining). The sensory neurons from the control side did not show any staining for ATF3, while the experimental side showed ATF3 staining to a variable, but low extent (Table 5), with differences between the groups ($p = 0.002$; Kruskal–Wallis; for details of analysis see Ref. [24]). A significantly higher percentage of ATF3 labeled sensory neurons were observed in DRGs from CFeCNG^{2nd} rats, particularly in diabetic rats (Table 5).

3.2.2.2. Degree of neuroprotection (HSP27-staining). Accordingly, HSP27 was observed in DRG from the control side with around 18.0–22.4% of the area stained without any difference between the groups (Table 5), while the staining on the experimental side was significantly higher ($p = 0.0001$ Wilcoxon). Furthermore, a significant difference between the experimental groups was observed concerning the HSP27 staining (Table 5); the expression of HSP27 on the experimental side was again higher in the DRGs from the diabetic GK rats (Fisher test values; Table 5), without a general difference between the two types of nerve guides. Accordingly, the HSP27 expression ratio (i.e. experimental/control) revealed also differences

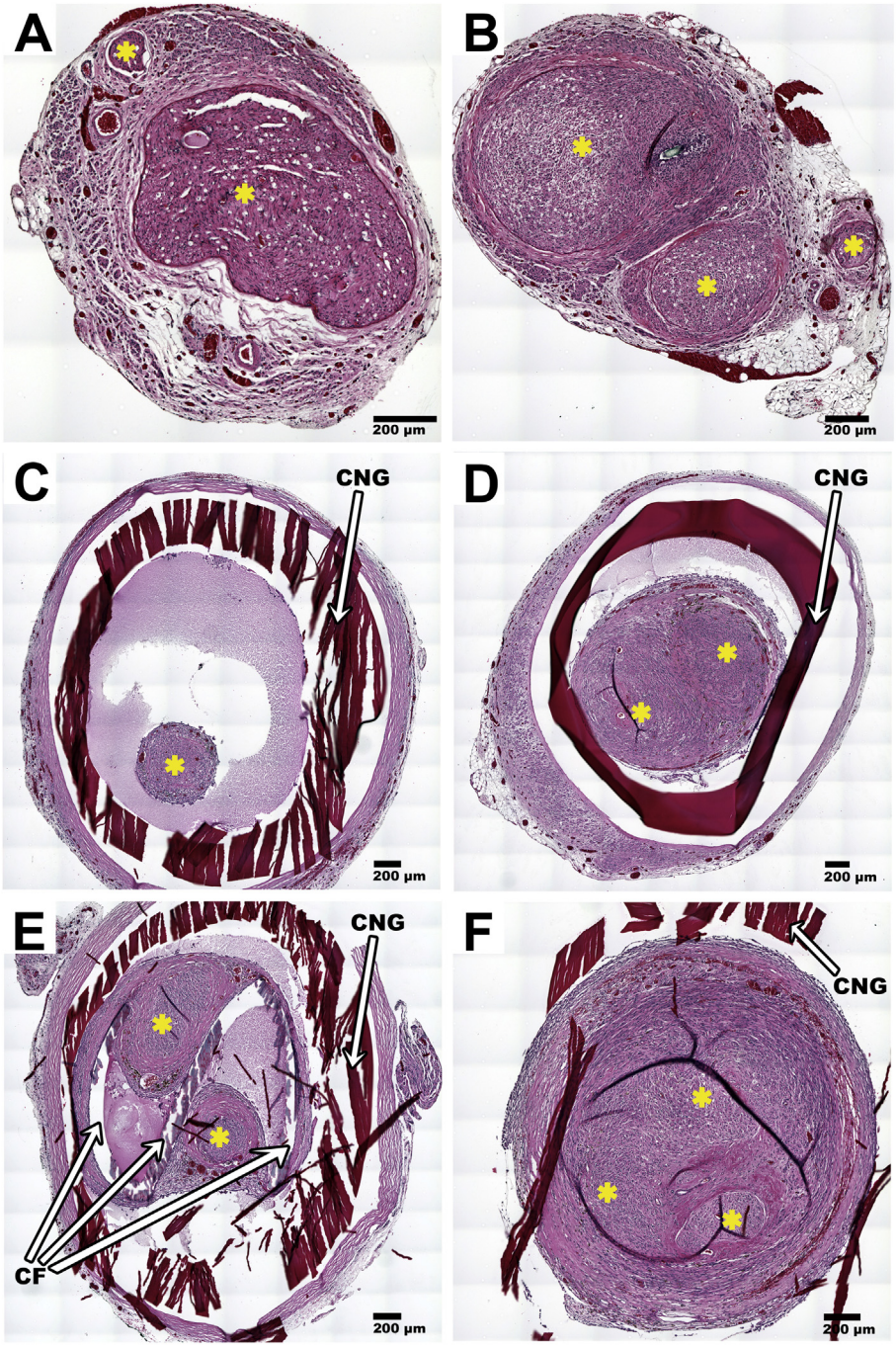

Fig. 6. Representative photomicrographs acquired from histological cross sections obtained at mid-graft level (A,C,E) or at ~1 mm proximal to the distal suture (B,D,F). Sections have been taken from samples of the ANG group (A,B), the hCNG-III group (C,D), and the CFeCNG^{2nd} group (E,F). Nerve fascicles identified in the HE staining are marked with yellow asterisks. (A) At mid-graft level an ANG is comprised of one large and one small nerve fascicle, (B) while it is separated into three fascicles in the distal region. (C) At mid-graft level a thin free floating tissue cable is detectable in hCNG-III, (D) which becomes thicker and separated into more than one fascicle at the distal region. (E) Two tissue cables separated by a z-shaped CF are visible at the mid-graft region of CFeCNG^{2nd} grafts. (F) The separate tissue cables then fuse to form a single bigger cable containing several nerve fascicles. CNG: chitosan nerve guide, CF: chitosan film.

between the groups ($p = 0.013$; Kruskal–Wallis) and with significantly higher values in the CFeCNG^{2nd} and in the diabetic GK rats (Fisher's test values; Table 5).

4. Discussion

Various conduit designs considering different intraluminal guidance structures have been experimentally examined for reconstruction of peripheral nerve defects [1]. Despite the diversity of these designs, however, little progress has been made in approving a product for clinical use that is able to reach the level of recovery seen when using the clinical standard treatment (autologous nerve grafting), especially if the nerve defect exceeds a critical length of 3 cm in humans [2,4,8]. Consequently, autologous nerve grafting still remains the surgeons preferred choice for bridging extended defects between two nerve ends, because this method gives at least a minimum chance for some functional recovery depending on the reconstructed nerve trunk [3]. Several

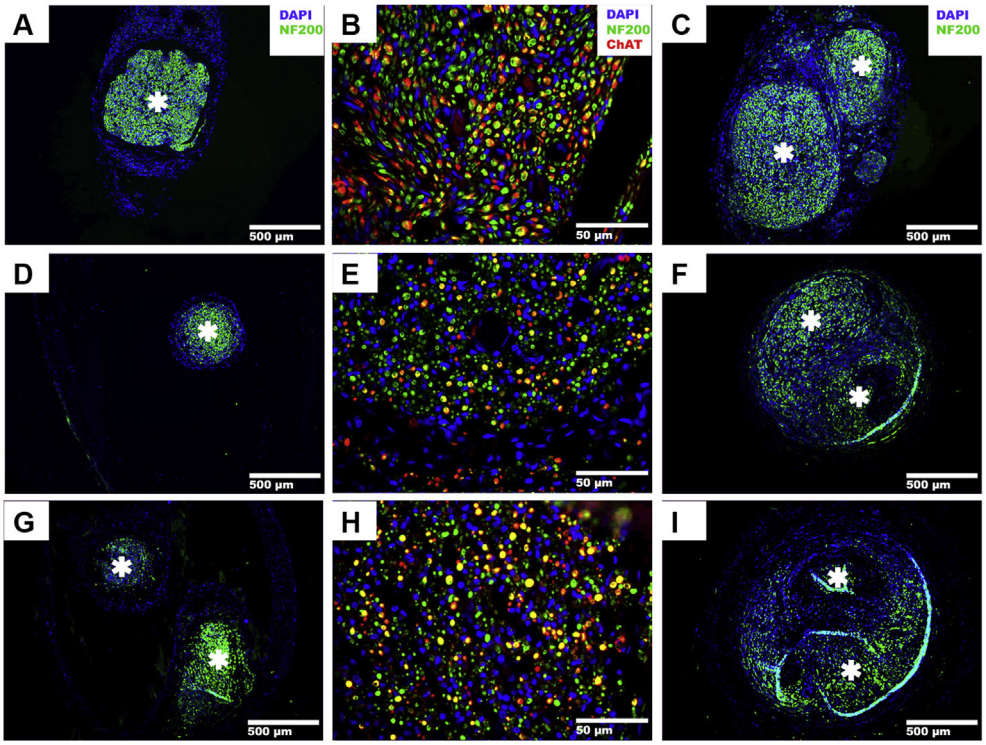

Fig. 7. Representative photomicrographs acquired from histological cross sections double-stained for neurofilament (NF200, green) and acetylcholine transferase (ChAT, red) and counterstained with DAPI (blue). The sections have been taken from samples of the ANG group (A–C), the hCNG-III group (D–F), and the CFeCNG^{2nd} group (G–I) at mid-graft level (A,D,G) or at ~1 mm proximal to the distal suture (C,F,I). White asterisks mark NF-200 immunopositive areas (nerve fascicles). (B,E,H) Merge and magnifications of the three immunostainings demonstrating nerve fascicle details and the contained regenerated motor axons (yellow).

attempts have been made to develop effective alternatives for autologous nerve grafting and promising results have been achieved experimentally and some even applied clinically, such as processed nerve allografts [26–28]. For example, non-biodegradable poly-sulfon nerve guides enhanced with one electrospun aligned thin film (poly-acrylonitril-co-methylacrylate) within their lumen were reported to significantly increase peripheral nerve regeneration across a 14 mm rat sciatic nerve defect [20]. While these nerve guides have not yet been further advanced for a possible clinical application, other attempts were made to enhance already approved nerve guide devices with engineered neural tissue [29]. For the latter, approved NeuraWrap™ nerve guides were filled with engineered neural tissue containing adipose derived stem cells and demonstrated to support axonal regeneration across a 15 mm rat sciatic nerve defect in a short-term period of 8 weeks after reconstruction to a similar extent than autologous nerve grafts [29]. Although promising, the neural engineered tissue and the use of stem cells are not likely to overcome the regulatory burden for clinical use in the near future and also the functional outcome of regeneration remains to be investigated for this type of bioartificial graft. In the recent years only one engineered nerve guide with intraluminal structures has been translated into a clinical investigation, the Neuromaix nerve guide [30] but results are not yet published. This nerve guide is collagen based and composed of an outer shell conduit filled with an inner sponge-like conduit, for which the support of functional recovery across a 2 cm rat sciatic nerve defect has already been demonstrated [31].

In the present study we evaluated chitosan films as alternative guidance substrate for regenerating axons within chitosan nerve guides across an extended rat sciatic nerve defect (15 mm). The basic chitosan nerve guides have already been approved for clinical use in Europe (CE mark, Reaxon® Nerve Guide). This was achieved after demonstrating their very good pro-regenerative properties in rat models evaluating standard and critical length nerve defect reconstruction [15–18]. These nerve guides further provide a high mechanical strength and collapse stability combined with transparency and easiness to suture them with microneedles [15], thus making it very likely that these off-the-shelve nerve guides will be widely accepted when autologous nerve grafting is not the first option for the surgeon or the patient. The chitosan films used in the present study to enhance the hollow chitosan nerve guides (hCNGs) are made under equal ISO standard protocols and out of the same certified medical grade chitosan. Therefore, only a short period will be needed until the equally transparent and collapse stable chitosan film enhanced chitosan nerve guides (CFeCNGs) may be available for clinical use. With the present results, we show that CFeCNGs significantly improved nerve regeneration for critical length defect reconstruction compared to hCNGs. Furthermore, this higher pro-regenerative effect has been demonstrated not only in healthy, but also in diabetic rats in which clinically relevant blood glucose profiles were measured.

The chitosan films were thought to support the fibrin matrix, which is initially formed upon injury and nerve guide aided nerve repair [32–34]. Importantly, it is most likely that the incomplete formation of this fibrin-based cable, or even the lack of formation, causes failure of regeneration across large defects [2,35]. Within one week after bridging a 10 mm defect, the fibrin-based cable connects the two nerve stumps and Schwann cells start to migrate along it and proliferate to form the bands of Büngner before axonal sprouts can cross the defect in the axonal phase [2,15,32,34]; again with a successful axonal outgrowth in diabetic GK rats [17].

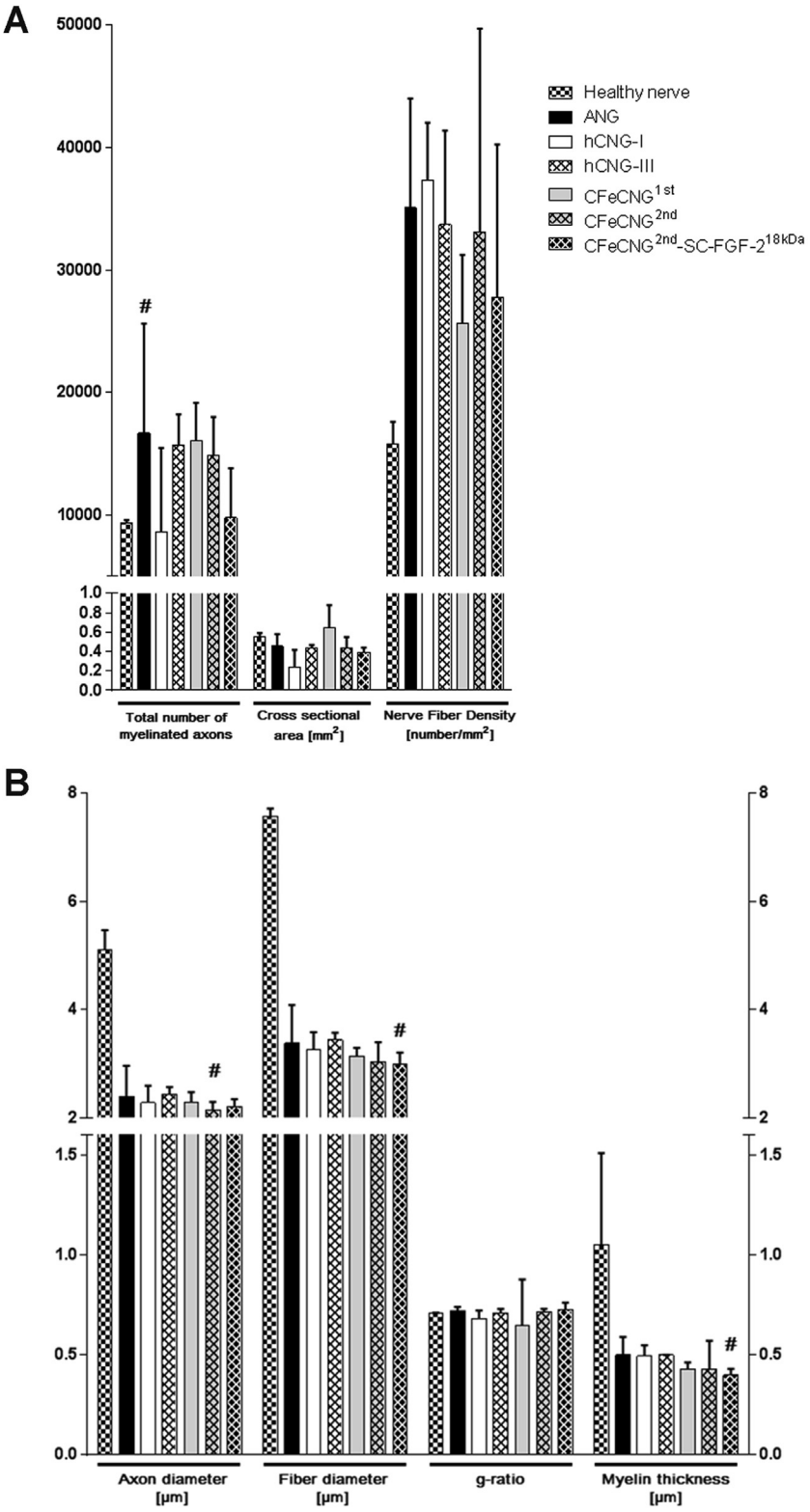

Fig. 8. Results of the morphometric analysis of the distal nerve, 5 mm distal to the nerve guide or graft, from Study I and Study III. (A) Total number of regenerated myelinated axons, total cross sectional area [mm^2], and calculated nerve fiber density. (B) Parameters related to axonal maturation: axon diameter, fiber diameter, g-ratio, and myelin thickness. Data are given in median ± range. Number of analyzed specimens: n = 3: healthy nerve and hCNG-III; n = 4: hCNG-I and $CFeCNG^{1st}$; n = 6: $CFeCNG^{2nd}$ and $CFeCNG^{2nd}$-SC-$FGF\text{-}2^{18kDa}$; n = 8: ANG. Results were tested for significance ($p < 0.05$) using Kruskal–Wallis test, followed by Dunn's multiple comparison. #$p < 0.05$ vs contralateral healthy nerve.

Importantly, it is considered that the absent or incomplete formation of this fibrin-based cable causes failure of regeneration across long defects [2,35]. Within one week after bridging a 10 mm defect in the rat sciatic nerve, the fibrin-based cable connects the two nerve stumps, providing physical support to the migration of fibroblasts and Schwann cells along it before axonal sprouts can cross the gap in the axonal phase [2,15,32]. In the present study where a 15 mm sciatic nerve defect was bridged with hCNGs or

Table 3
Blood glucose levels in healthy and diabetic Goto-Kakizaki (GK) rats evaluated for up to 56 days post surgery in study II. Values are median [25th (Q1) – 75th (Q3) percentiles].

		hCNG-II^{healthy}	CFeCNG$^{2nd\text{-}healthy}$	hCNG-II^{diabetic}	CFeCNG$^{2nd\text{-}diabetic}$	p-values (KW[a])	Fisher's method[b]	
							hCNG-II/CFeCNG^{2nd}	Healthy rats/ Diabetic rats
B-glucose (mmol/l)	preoperative	4.0 [3.6–4.4]	3.6 [3.3–4.0]	8.7 [8.1–1.2]	7.9 [7.4–8.4]	0.0001	0.68	<0.0001
	postoperative	4.1 [3.8–4.49]	4.3 [4.0–4.6]	9.0 [7.7–11.2]	7.7 [7.5–8.7]	0.0001	0.27	<0.0001

[a] KW = Kruskal–Wallis.
[b] Fisher method for independent samples based on the chi square distribution.

Table 4
Nerve regeneration in healthy and diabetic Goto-Kakizaki (GK) rats evaluated 56 days post surgery in study II. Values are median [25th (Q1) –75th (Q3) percentiles].

		hCNG-II^{healthy}	CFeCNG$^{2nd\text{-}healthy}$	hCNG-II^{diabetic}	CFeCNG$^{2nd\text{-}diabetic}$	p-values (KW[a])	Fisher's method[b]	
							hCNG-II/ CFeCNG^{2nd}	Healthy rats/ Diabetic rats
Presence of axons (neurofilament staining; animals/group)	In nerve guide	6/8	8/8	6/8	8/8	0.21[#]	NA	NA
	In distal nerve	3/8	8/8	4/8	8/8	0.005[#]	0.01	1.00
ATF3 - + Schwann cells (% of total)	At 3 mm	0.9 [0.5–1.5]	1.5 [1.4–2.7]	0.9 [0.4–1.9]	2.7 [2.3–3.0]	**0.004**	**0.008**	0.19
	In nerve guide	0.8 [0.7–1.2]	2.8 [2.1–3.0]	1.7 [1.5–2.0]	3.7 [3.0–4.3]	**0.0001**	**<0.0001**	**0.0002**
	In distal nerve	1.8 [1.2–3.3]	5.0 [3.9–5.3]	5.4 [4.2–6.3]	7.6 [7.0–10.5]	**0.0001**	**<0.0001**	**<0.0001**
Cleaved caspase-3 - + Schwann cells (% of total)	At 3 mm	2.6 [1.8–2.8]	4.6 [4.3–5.4]	3.9 [3.4–4.4]	4.8 [4.6–5.4]	**0.0001**	**0.0001**	**0.0006**
	In nerve guide	1.6 [1.3–2.3]	2.2 [1.9–2.6]	3.8 [3.5–4.5]	3.6 [3.3–3.9]	**0.0001**	0.094	**<0.0001**
	In distal nerve	8.7 [8.2–9.3]	7.6 [7.0–8.1]	7.9 [7.6–8.5]	6.9 [6.4–7.4]	**0.0001**	**0.0002**	**0.013**
DAPI stained cells (no/mm^2)	At 3 mm	862 [806–903]	1016 [999–1063]	1090 [1072–1106]	1070 [1062–1130]	**0.0001**	**<0.0001**	**<0.0001**
	In nerve guide	775 [759–796]	923 [904–988]	871 [852–885]	966 [951–987]	**0.0001**	**<0.0001**	**<0.0001**
	In distal nerve	1038 [1023–1107]	1051 [1035–1078]	1069 [1057–1089]	1010 [940–1204]	0.57	NA	NA

+ = Immunopositive.
NA = Not applicable.
At 3 mm = 3 mm distal to the proximal suture line. In nerve guide = in center of nerve guide. [#] indicates overall Chi-squared test (Pearson Chi-squared, cross tabulation > 2 × 2). The Fishers's method for neurofilament staining is based on subsequent 2 × 2 cross tabulation Fisher's exact test.
p-values indicating significant differences are set in bold.
[a] KW = Kruskal–Wallis.
[b] Fisher method for independent samples based on the chi square distribution.

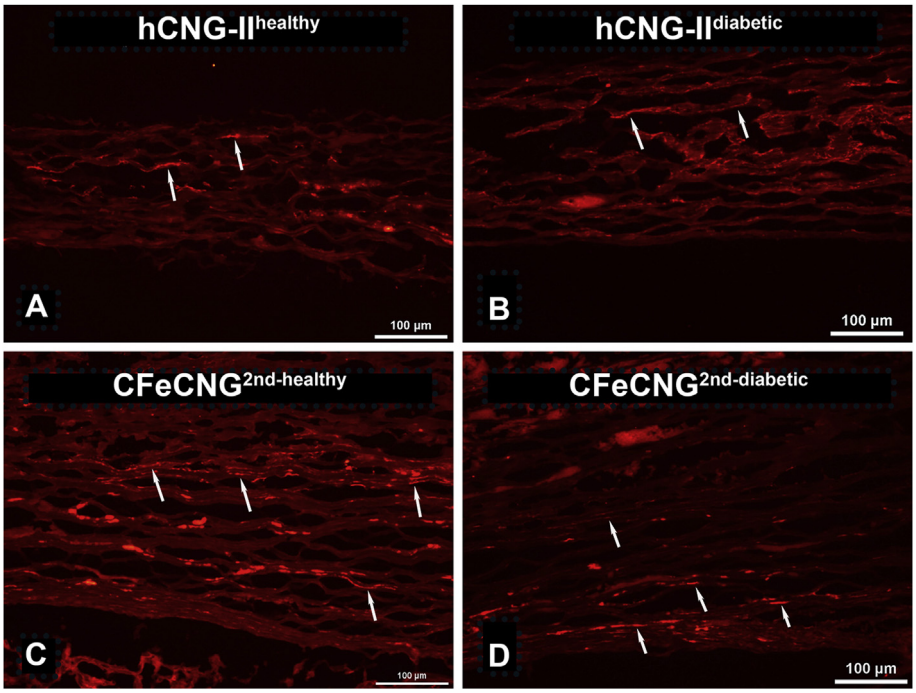

Fig. 9. Neurofilament staining in the formed matrix in healthy (A,C) and diabetic GK (B, D) rats repaired with hCNG (A, B) and with CFeCNG^{2nd} (C,D) nerve guides at 56 days post surgery. Axons (arrows) were present in all CFeCNG^{2nd} nerve guides (8/8 healthy and 8/8 GK rats) as well as in nerve guides of 6/8 hCNG-II^{healthy} and 6/8 hCNG-II^{diabetic} rats. Scale bar = 100 µm.

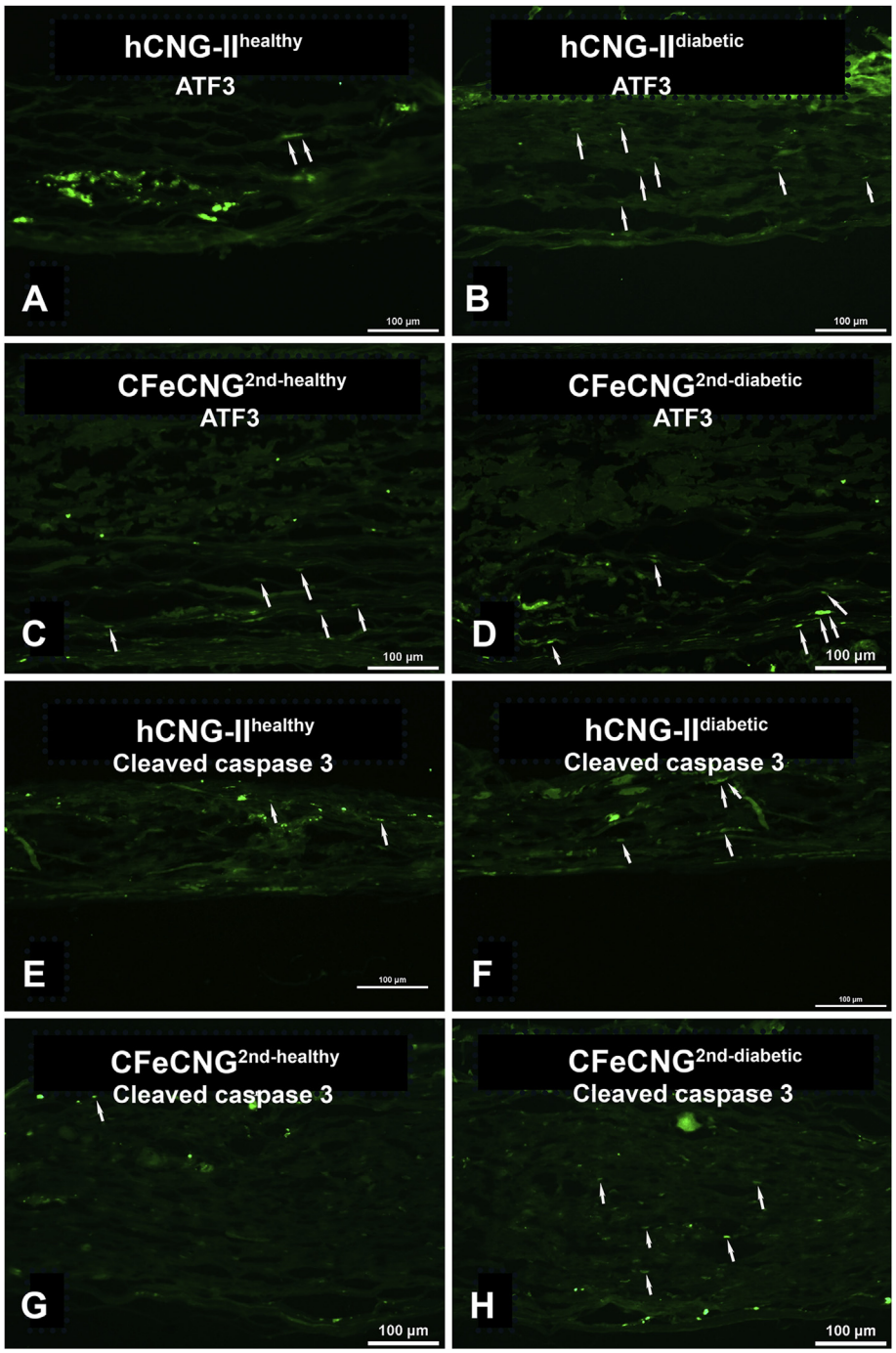

Fig. 10. Staining for activating transcription factor 3 (ATF3) (A–D) and cleaved caspase 3 (E–H) in the formed matrix in healthy (A, C, E, G) and diabetic GK (B, D, F, H) rats reconstructed with hCNG (A, B, E, F) or CFeCNG^{2nd} (C, D, G, H) at 56 days post surgery. Arrows indicate stained oval shaped Schwann cells. Scale bar = 100 µm.

CFeCNGs, a substantial regenerative matrix was found in the samples taken at 56 days after surgery in both healthy and diabetic rats. Importantly, the quality of the formed matrix was improved in the CFeCNG treated animals, and regenerating axons had already reached the distal nerve segment in a significantly higher proportion at 56 days after surgery, allowing muscle reinnervation detectable in some cases at 60 days. Furthermore, the regenerative matrix as well as the nerve segment just distal to the implanted CFeCNG displayed significantly increased numbers of activated Schwan cells (ATF3-immunopositive), which are likely to attract regrowing axons [7,15,24]. Simultaneously, the apoptotic events, as indicated by cleaved caspase 3 immunopositive Schwann cells, were reduced in nerve segments distal to CFeCNG implants, indicating that also events potentially deleterious for axonal regeneration [15] are reduced. The support of axonal regeneration by CFeCNG is further strengthened by the interesting finding that a higher number of sensory DRG neurons were found, i.e. ATF3 stained, as well as a larger area was stained for HSP27, as an indicator for increased neuroprotection [6], particularly in the diabetic GK rats with a moderately increased blood glucose level. It is conclusive that a higher degree of neuronal protection and activation together with a higher degree of Schwann cell activation and

Table 5
Analysis of sensory dorsal root ganglia (L4-L5) in healthy and diabetic Goto-Kakizaki (GK) rats evaluated 56 days post surgery in study II. Values are median [25th (Q1) – 75th (Q3) percentiles].

		hCNG-II^{healthy}	CFeCNG$^{2nd\text{-}healthy}$	hCNG-II^{diabetic}	CFeCNG$^{2nd\text{-}diabetic}$	p-values (KW[a])	Fisher's method[b]	
							hCNG-II/ CFeCNG^{2nd}	Healthy rats/ Diabetic rats
ATF3- + - cells (% of total)	Experimental	6.4 [3.9–7.1]	6.9 [5.8–11.9]	6.5 [5.5–8.7]	14.4 [13.3–20.0]	**0.002**	**0.003**	**0.01**
HSP27 expression (% of area)	Control	21.3 [18.4–22.8]	18.1 [16.8–20.4]	22.4 [19.0–23.9]	18.0 [16.6–19.7]	0.13	NA	NA
	Experimental	27.4 [24.8–29.4]	27.3 [25.5–30.5]	30.2 [24.5–32.3]	34.1 [32.1–35.9]	**0.023**	0.17	**0.03**
HSP27 Ratio (experimental/control)		1.35 [1.27–1.54]	1.62 [1.28–1.79]	1.25 [1.10–1.61]	1.83 [1.61–2.13]	**0.013**	**0.003**	**0.01**

+ = Immunopositive.
NA = Not applied.
p-values indicating significant differences are set in bold.
[a] KW = Kruskal–Wallis.
[b] Fisher method for independent samples based on the chi square distribution.

reduced apoptosis during the early phase of regeneration can lead to better functional recovery in the long term.

Usually, when new types of nerve guides or tissue engineered nerve prostheses are developed, the general health condition of the tested animals is not considered. The globally increasing number of patients with diabetes, however, makes it crucial to develop peripheral nerve reconstruction treatment strategies also suitable for patients in which neuropathies often occur [7]. Here, we demonstrate that during the matrix phase axonal regeneration is equally supported in healthy and diabetic GK rats after critical nerve defect reconstructed with CFeCNG^{2nd}. With regard to the processes undergoing in the corresponding DRGs, it has been demonstrated earlier that HSP27 is an important factor preserving nerve function in diabetic patients [23]. Here we also demonstrate that the HSP27 expression together with that of ATF3 has been found to be increased in DRGs from diabetic GK rats. In diabetic GK rats, the regenerative matrix within the nerve guides contained higher numbers of cells in general and of activated (ATF3-immunopositive) Schwann cells in particular. With regard to apoptotic events in Schwann cells we found that those are increased within the regenerative matrix but not in the distal nerve segments in diabetic GK rats. In contrast, it has been demonstrated earlier that Schwann cells in diabetic animals are less responsive to a nerve injury [36] and that nerves in diabetic animals have a slower regeneration after end-to-end repair [6]. Therefore the results obtained in the present study notably indicate that peripheral nerve reconstruction by means of basic or enhanced chitosan nerve guides represents a promising alternative to standard treatments in diabetic rats with clinically relevant blood glucose levels.

The pro-regenerative properties of chitosan are well documented not only for the peripheral and the central nervous system but also for other applications in regenerative medicine and wound healing [37–39]. Beside its antimicrobial properties also the angiogenic properties of chitosan materials are important in the context of regenerative medicine. Indeed, we observed robust neovascularization not only in the short term, being even more evident in the diabetic animals, but also on the long term, where exclusively in the second generation CFeCNGs (with perforated chitosan films) small blood vessels traveling through the holes in the chitosan films were visible. Angiogenesis is important for the survival of cells and tissue and crucial for the success of peripheral nerve regeneration across a critical length [40]. In the present study, long term axonal regeneration, as determined by nerve morphometry, was similar among all nerve guide conditions examined. When it comes to functional nerve recovery, however, the introduction of perforated chitosan films in CFeCNGs was sufficient to further increase the functional outcome compared to hCNGs. The latter was clearly demonstrated by electrophysiological recording of muscle reinnervation at 120 days after surgery. Implantation of CFeCNGs to bridge the 15 mm sciatic nerve defect induced higher reinnervation rates of the TA and PL muscles. The success rates increased by 20–30% in the CFeCNG^{2nd} group (perforated chitosan film) compared to the CFeCNG^{1st} group (continuous chitosan film). Regarding the outcome of sensory recovery in the present study at 120 days after surgery, study I revealed less efficiency of implantation of CFeCNG^{1st} compared to that of hCNG. In contrast, study III revealed the opposite and most similar recovery in comparison to autologous nerve grafting for the CFeCNG^{2nd} group. Thus, it can be hypothesized that the perforations within the chitosan films allowed nutrient interchange between the two sub-compartments within the second generation CFeCNGs (also via capillaries connecting the regenerative tissue along both sides of the chitosan films). This condition probably supported cell migration and survival across the nerve defect and formation of the regenerative fibrin matrix to a higher extent than non-perforated chitosan films used in first generation CFeCNG. Subsequently 15 mm nerve defect reconstruction with second generation CFeCNGs resulted in even increased functional recovery.

In study III we included an additional condition, the enrichment of CFeCNG^{2nd} with FGF-2^{18kDa} overexpressing Schwann cells (SC-FGF-2^{18kDa}). It was earlier demonstrated that these cells increase functional recovery across 15 mm sciatic nerve defects [41] and even support it when the regeneration process is impaired by local obstacles such as a too dense hydrogel within chitosan nerve guides [19]. In the present study CFeCNG^{2nd}-SC-FGF-2^{18kDa}did not further increase the regeneration outcome. The functional recovery was rather less in comparison to the implantation of cell free CFeCNG^{2nd}. This indicates that although Schwann cell survival within the nerve guides previously has been proven in vitro and neovascularization for nutrient supply in vivo was detectable, the implanted Schwann cells did not likely survive in vivo and their debris and metabolites might also interfere with the regrowth of axons. The Schwann cells have been seeded on non-coated chitosan films because this has been evaluated previously in vitro [21]. However, in previous studies, where they demonstrated to be effective, the cells had been suspended in different types of hydrogels [19,41,42]. Future attempts have to be made to ensure survival of Schwann cells seeded into CFeCNGs.

5. Conclusions

In the present study, hollow chitosan nerve guides were enhanced by introduction of chitosan films to increase the regeneration outcome across peripheral sciatic nerve defects of critical length, i.e. 15 mm, in healthy and diabetic rats. This enhanced chitosan nerve guides not only supported robust axonal

regeneration and functional recovery in healthy animals but also demonstrated to be beneficial for the regeneration process in diabetic rats with relevant blood glucose levels. Thus, we have an effective peripheral nerve regenerative device at hand, which represents an ideal candidate for the translation into the clinic. All components of the enhanced nerve guides can be produced under ISO standards. Furthermore, the maintained transparency and the easiness to suture the device between the nerve ends are likely to facilitate its wide acceptance among nerve surgeons. Based on the results presented here, future experiments can now proceed to address even more complex and challenging conditions for peripheral nerve reconstruction and recovery, such as the common conditions of delayed repair or the reconstruction across joints, e.g. in digital nerve repair.

Acknowledgments

This study was supported by the European Community's Seventh Framework Programme (FP7-HEALTH-2011) under grant agreement nº 278612 (BIOHYBRID). Medical grade chitosan for manufacturing the chitosan films and nerve guides was supplied by Altakitin SA (Lisbon, Portugal). The chitosan materials were supplied by Medovent GmbH (Mainz, Germany). The authors thank Dr. Andreas Ratzka, Institute of Neuroanatomy, for the construction of the plasmids used in this study. We thank Professor Jonas Björk, Lund University, Lund, Sweden for statistical advice of the Fisher's method. We are further thankful to Silke Fischer, Natascha Heidrich, Jennifer Metzen, Hildegard Streich, Maike Wesemann (all Institute of Neuroanatomy, Hannover Medical School), to Monica Espejo, Jessica Jaramillo and Marta Morell (Universitat Autonoma de Barcelona) for their technical support.

References

[1] X. Gu, F. Ding, D.F. Williams, Neural tissue engineering options for peripheral nerve regeneration, Biomaterials 35 (2014) 6143–6156.
[2] W. Daly, L. Yao, D. Zeugolis, A. Windebank, A. Pandit, A biomaterials approach to peripheral nerve regeneration: bridging the peripheral nerve gap and enhancing functional recovery, J. R. Soc. Interface 9 (2012) 202–221.
[3] R. Deumens, A. Bozkurt, M.F. Meek, M.A. Marcus, E.A. Joosten, J. Weis, et al., Repairing injured peripheral nerves: bridging the gap, Prog. Neurobiol. 92 (2010) 245–276.
[4] R.A. Weber, W.C. Breidenbach, R.E. Brown, M.E. Jabaley, D.P. Mass, A randomized prospective study of polyglycolic acid conduits for digital nerve reconstruction in humans, Plast. Reconstr. Surg. 106 (2000) 1036–1045 discussion 46–8.
[5] A. Faroni, S.A. Mobasseri, P.J. Kingham, A.J. Reid, Peripheral nerve regeneration: experimental strategies and future perspectives, Adv. Drug Deliv. Rev. 82–83 (2015) 160–167.
[6] L. Stenberg, L.B. Dahlin, Gender differences in nerve regeneration after sciatic nerve injury and repair in healthy and in type 2 diabetic Goto-Kakizaki rats, BMC Neurosci. 15 (2014) 107.
[7] L. Stenberg, M. Kanje, K. Dolezal, L.B. Dahlin, Expression of activating transcription factor 3 (ATF 3) and caspase 3 in Schwann cells and axonal outgrowth after sciatic nerve repair in diabetic BB rats, Neurosci. Lett. 515 (2012) 34–38.
[8] J.H. Bell, J.W. Haycock, Next generation nerve guides: materials, fabrication, growth factors, and cell delivery, Tissue Eng. Part B Rev. 18 (2012) 116–128.
[9] M.E. Boeckstyns, A.I. Sorensen, J.F. Vineta, B. Rosen, X. Navarro, S.J. Archibald, et al., Collagen conduit versus microsurgical neurorrhaphy: 2-year follow-up of a prospective, blinded clinical and electrophysiological multicenter randomized, controlled trial, J. Hand Surg. Am. 38 (2013) 2405–2411.
[10] G. Lundborg, B. Rosen, S.O. Abrahamson, L. Dahlin, N. Danielsen, Tubular repair of the median nerve in the human forearm. Preliminary findings, J. Hand Surg. Br. 19 (1994) 273–276.
[11] G. Lundborg, B. Rosen, L. Dahlin, J. Holmberg, I. Rosen, Tubular repair of the median or ulnar nerve in the human forearm: a 5-year follow-up, J. Hand Surg. Br. 29 (2004) 100–107.
[12] X. Wang, W. Hu, Y. Cao, J. Yao, J. Wu, X. Gu, Dog sciatic nerve regeneration across a 30-mm defect bridged by a chitosan/PGA artificial nerve graft, Brain 128 (2005) 1897–1910.
[13] C. Xue, N. Hu, Y. Gu, Y. Yang, Y. Liu, J. Liu, et al., Joint use of a Chitosan/PLGA scaffold and MSCs to bridge an extra large gap in dog sciatic nerve, Neurorehabil Neural Repair 26 (2012) 96–106.
[14] F. Ding, J. Wu, Y. Yang, W. Hu, Q. Zhu, X. Tang, et al., Use of tissue-engineered nerve grafts consisting of a Chitosan/Poly(lactic-co-glycolic acid)-based scaffold included with bone marrow mesenchymal cells for bridging 50-mm dog sciatic nerve gaps, Tissue Eng. Part A 16 (2010) 3779–3790.
[15] K. Haastert-Talini, S. Geuna, L.B. Dahlin, C. Meyer, L. Stenberg, T. Freier, et al., Chitosan tubes of varying degrees of acetylation for bridging peripheral nerve defects, Biomaterials 34 (2013) 9886–9904.
[16] Y. Shapira, M. Tolmasov, M. Nissan, E. Reider, A. Koren, T. Biron, et al., Comparison of results between chitosan hollow tube and autologous nerve graft in reconstruction of peripheral nerve defect: an experimental study, Microsurgery (2015 Apr 22), http://dx.doi.org/10.1002/micr.22418 (EPub ahead of print).
[17] L. Stenberg, A. Kodama, C. Lindwall-Blom, L.B. Dahlin, Special issue in the European journal of neuroscience nerve regeneration in chitosan conduits and in autologous nerve grafts in healthy and in type 2 diabetic Goto-Kakizaki rats, Eur. J. Neurosci. (2015), http://dx.doi.org/10.1111/ejn.13068. Epub ahead of print.
[18] F. Gonzalez-Perez, S. Cobianchi, S. Geuna, C. Barwig, T. Freier, E. Udina, et al., Tubulization with chitosan guides for the repair of long gap peripheral nerve injury in the rat, Microsurgery 35 (2015) 300–308.
[19] C. Meyer, S. Wrobel, S. Raimondo, S. Rochkind, C. Heimann, A. Shahar, et al., Peripheral nerve regeneration through hydrogel enriched chitosan conduits containing engineered Schwann cells for drug delivery, Cell Transpl. (2015 Apr 14), http://dx.doi.org/10.3727/096368915X688010 (EPub ahead of print).
[20] I.P. Clements, Y.T. Kim, A.W. English, X. Lu, A. Chung, R.V. Bellamkonda, Thin-film enhanced nerve guidance channels for peripheral nerve repair, Biomaterials 30 (2009) 3834–3846.
[21] S. Wrobel, S.C. Serra, S. Ribeiro-Samy, N. Sousa, C. Heimann, C. Barwig, et al., In vitro evaluation of cell-seeded chitosan films for peripheral nerve tissue engineering, Tissue Eng. Part A 20 (2014) 2339–2349.
[22] Y. Tsuda, M. Kanje, L.B. Dahlin, Axonal outgrowth is associated with increased ERK 1/2 activation but decreased caspase 3 linked cell death in Schwann cells after immediate nerve repair in rats, BMC Neurosci. 12 (2011) 12.
[23] K. Pourhamidi, H. Skarstrand, L.B. Dahlin, O. Rolandsson, HSP27 concentrations are lower in patients with type 1 diabetes and correlate with large nerve fiber dysfunction, Diabetes Care 37 (2014) e49–50.
[24] H. Saito, L.B. Dahlin, Expression of ATF3 and axonal outgrowth are impaired after delayed nerve repair, BMC Neurosci. 9 (2008) 88.
[25] S. Cobianchi, J. de Cruz, X. Navarro, Assessment of sensory thresholds and nociceptive fiber growth after sciatic nerve injury reveals the differential contribution of collateral reinnervation and nerve regeneration to neuropathic pain, Exp. Neurol. 255 (2014) 1–11.
[26] B.D. Rinker, J.V. Ingari, J.A. Greenberg, W.P. Thayer, B. Safa, G.M. Buncke, Outcomes of short-gap sensory nerve injuries reconstructed with processed nerve allografts from a multicenter registry study, J. Reconstr. Microsurg 31 (2015) 384–390.
[27] M.S. Cho, B.D. Rinker, R.V. Weber, J.D. Chao, J.V. Ingari, D. Brooks, et al., Functional outcome following nerve repair in the upper extremity using processed nerve allograft, J. Hand Surg. Am. 37 (2012) 2340–2349.
[28] D.N. Brooks, R.V. Weber, J.D. Chao, B.D. Rinker, J. Zoldos, M.R. Robichaux, et al., Processed nerve allografts for peripheral nerve reconstruction: a multicenter study of utilization and outcomes in sensory, mixed, and motor nerve reconstructions, Microsurgery 32 (2012) 1–14.
[29] M. Georgiou, J.P. Golding, A.J. Loughlin, P.J. Kingham, J.B. Phillips, Engineered neural tissue with aligned, differentiated adipose-derived stem cells promotes peripheral nerve regeneration across a critical sized defect in rat sciatic nerve, Biomaterials 37 (2015) 242–251.
[30] A. Bozkurt, S.G. van Neerven, K.G. Claeys, D.M. O'Dey, A. Sudhoff, G.A. Brook, et al., The proximal medial sural nerve biopsy model: a standardised and reproducible baseline clinical model for the translational evaluation of bioengineered nerve guides, Biomed. Res. Int. 2014 (2014) 121452.
[31] A. Bozkurt, F. Lassner, D. O'Dey, R. Deumens, A. Bocker, T. Schwendt, et al., The role of microstructured and interconnected pore channels in a collagen-based nerve guide on axonal regeneration in peripheral nerves, Biomaterials 33 (2012) 1363–1375.
[32] J.S. Belkas, M.S. Shoichet, R. Midha, Peripheral nerve regeneration through guidance tubes, Neurol. Res. 26 (2004) 151–160.
[33] L.R. Williams, F.M. Longo, H.C. Powell, G. Lundborg, S. Varon, Spatial-temporal progress of peripheral nerve regeneration within a silicone chamber: parameters for a bioassay, J. Comp. Neurol. 218 (1983) 460–470.
[34] Q. Zhao, L.B. Dahlin, M. Kanje, G. Lundborg, Repair of the transected rat sciatic nerve: matrix formation within implanted silicone tubes, Restor. Neurol. Neurosci. 5 (1993) 197–204.
[35] Y.T. Kim, V.K. Haftel, S. Kumar, R.V. Bellamkonda, The role of aligned polymer fiber-based constructs in the bridging of long peripheral nerve gaps, Biomaterials 29 (2008) 3117–3127.
[36] L. Stenberg, M. Kanje, L. Martensson, L.B. Dahlin, Injury-induced activation of ERK 1/2 in the sciatic nerve of healthy and diabetic rats, Neuroreport 22 (2010) 73–77.
[37] K. Azuma, S. Ifuku, T. Osaki, Y. Okamoto, S. Minami, Preparation and biomedical applications of chitin and chitosan nanofibers, J. Biomed. Nanotechnol. 10 (2014) 2891–2920.
[38] M.B. Dreifke, A.A. Jayasuriya, A.C. Jayasuriya, Current wound healing procedures and potential care, Mater Sci. Eng. C Mater Biol. Appl. 48 (2015) 651–662.

[39] S. Gnavi, C. Barwig, T. Freier, K. Haastert-Talini, C. Grothe, S. Geuna, The use of Chitosan-based scaffolds to enhance regeneration in the nervous system, Int. Rev. Neurobiol. 109C (2013) 1–62.
[40] G. Penkert, W. Bini, M. Samii, Revascularization of nerve grafts: an experimental study, J. Reconstr. Microsurg 4 (1988) 319–325.
[41] K. Haastert, E. Lipokatic, M. Fischer, M. Timmer, C. Grothe, Differentially promoted peripheral nerve regeneration by grafted Schwann cells overexpressing different FGF-2 isoforms, Neurobiol. Dis. 21 (2006) 138–153.
[42] K. Haastert-Talini, J. Schaper-Rinkel, R. Schmitte, R. Bastian, M. Muhlenhoff, D. Schwarzer, et al., In vivo evaluation of polysialic acid as part of tissue-engineered nerve transplants, Tissue Eng. Part A 16 (2010) 3085–3098.